Title

Multimodal Imaging Mass Spectrometry: Next Generation Molecular Mapping in Biology and Medicine.

Journal

Journal of The American Society for Mass Spectrometry, 31(12)

Authors

Neumann, Elizabeth

Djambazova, Katerina

Caprioli, Richard

et al.

Publication Date

2020-12-02

DOI

10.1021/jasms.0c00232

Peer reviewed

HHS Public Access

Author manuscript

J Am Soc Mass Spectrom. Author manuscript; available in PMC 2022 July 13.

Published in final edited form as:

J Am Soc Mass Spectrom. 2020 December 02; 31(12): 2401–2415. doi:10.1021/jasms.0c00232.

Multimodal Imaging Mass Spectrometry: Next Generation Molecular Mapping in Biology and Medicine

Elizabeth K. Neumann,
Department of Biochemistry and Mass Spectrometry Research Center, Vanderbilt University, Nashville, Tennessee 37205, United States

Katerina V. Djambazova,
Mass Spectrometry Research Center and Department of Chemistry, Vanderbilt University, Nashville, Tennessee 37235, United States

Richard M. Caprioli,
Department of Biochemistry, Mass Spectrometry Research Center, Department of Pharmacology, Department of Chemistry, and Department of Medicine, Vanderbilt University, Nashville, Tennessee 37205, United States

Jeffrey M. Spraggins
Department of Biochemistry, Mass Spectrometry Research Center, and Department of Chemistry, Vanderbilt University, Nashville, Tennessee 37205, United States

Abstract

Imaging mass spectrometry has become a mature molecular mapping technology that is used for molecular discovery in many medical and biological systems. While powerful by itself, imaging mass spectrometry can be complemented by the addition of other orthogonal, chemically informative imaging technologies to maximize the information gained from a single experiment and enable deeper understanding of biological processes. Within this review, we describe MALDI, SIMS, and DESI imaging mass spectrometric technologies and how these have been integrated with other analytical modalities such as microscopy, transcriptomics, spectroscopy, and electrochemistry in a field termed multimodal imaging. We explore the future of this field and discuss forthcoming developments that will bring new insights to help unravel the molecular complexities of biological systems, from single cells to functional tissue structures and organs.

Graphical Abstract

Corresponding Author: Jeffrey M. Spraggins – Department of Biochemistry, Mass Spectrometry Research Center, and Department of Chemistry, Vanderbilt University, Nashville, Tennessee 37205, United States; Jeff.Spraggins@vanderbilt.edu.

Complete contact information is available at: https://pubs.acs.org/10.1021/jasms.0c00232

The authors declare no competing financial interest.

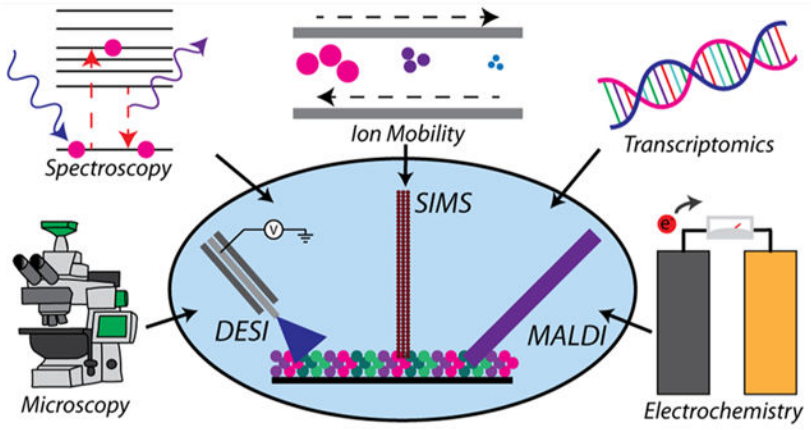

Keywords

imaging mass spectrometry; chemical imaging; multimodal analysis; tissue analysis

1. INTRODUCTION

Imaging mass spectrometry (IMS) is a technology that enables the mapping of hundreds to thousands of molecules within biological systems.[1–6] The instruments within the field can measure a diverse array of sample types and chemical classes, ranging from low molecular weight metabolites[7–10] and signaling molecules[11–13] to lipids,[14–21] peptides,[22–24] and proteins.[25–29] A typical IMS experiment involves defining an area of the sample surface to be imaged followed by the desorption and ionization at multiple discrete locations. Each desorbed location, or pixel, is composed of an individual mass spectrum. A molecular image is generated for each signal recorded by plotting the ion intensity of that signal throughout the array of pixels generated from the sample. While there are many types of IMS technologies that have been reported in literature, we highlight here the three most common: matrix-assisted laser desorption/ionization (MALDI),[30,31] secondary ion mass spectrometry (SIMS),[32–34] and desorption electrospray ionization (DESI).[35–38] Additional information on other types of IMS technologies can be found in several recent reviews.[1,4,39]

Each IMS technology can be coupled to a variety of analytical approaches to enhance the information gained in a single experiment. Although IMS provides rich, chemically informative spectra and mapping capabilities, combining this unique mass specific technology with other analytical approaches can provide additional information for an analyzed sample. Combining two or more imaging modalities is termed multimodal imaging. The accrued advantages include enhanced discrimination between modality specific chemical and instrumental noise from biologically relevant chemical signals, improved sensitivity and specificity of chemical classes not easily analyzed by a single modality alone, and enhanced data mining capabilities. Combining IMS technologies with other analytical approaches provides a more effective means to probe the molecular complexity of biological systems. In this review, we summarize major advancements in the

field of multimodal imaging mass spectrometry over the past few years and discuss the exciting future of this field.

2. OVERVIEW OF IMAGING MASS SPECTROMETRY TECHNOLOGIES

2.1. Matrix-Assisted Laser Desorption/Ionization.

MALDI is a common ionization method within the IMS field as it can visualize numerous molecular species over a broad mass range with great molecular diversity. For tissue analysis, sample preparation typically involves sectioning of tissues and thaw mounting these sections onto a glass slide or other target (e.g., conductive surface for high voltage ion sources) and subsequent application of an organic chemical matrix that aids in analyte desorption and ionization.[40] Spatial resolution is defined by the ablation area of the laser and the distance between pixels (pitch). A variety of matrices are used for specific molecular classes. Commonly used matrices include 2,5-dihydroxybenzoic acid[41] or cyano-4-hydroxycinnamic acid[42] for positive ion mode analysis of metabolites, lipids, and peptides. Additionally, 9-aminoacridine[43] is typically used for negative ion mode analysis of metabolites, lipids, and proteins, while 1,5-diaminonaphthalene[44] is employed for analysis of lipids in both ion polarities. Recently norharmane has been shown to be effective for the analysis of hydrophobic molecules and low molecular weight metabolites.[45] Matrix deposition is often performed robotically to best balance reproducibility, analyte extraction, achieve small crystal size, and produce coating homogeneity, although sublimation, sieving, and airbrushing are also used in the field.[4,46]

As high spatial resolution MALDI IMS capabilities are developed that approach cellular and subcellular resolutions, challenges in sensitivity arise as the number of molecules sampled decreases with smaller pixel sizes. Ultimately, spatial resolution is dependent upon multiple factors such as matrix crystal size, laser focus, and stage motor step precision. Most modern MALDI IMS platforms utilize either a frequency tripled Nd:YAG (355 nm) or nitrogen gas laser (337.7 nm) and can achieve spatial resolutions of 5–20 μm using traditional front-side laser optics.[50–52] Improving laser focus beyond 5 μm can be achieved with more advanced setups using lower laser wavelengths (e.g., 213 nm) or changing laser geometries (e.g., transmission-mode), to minimize the effective spot size as described in the next several examples. For instance, Heiles et al. demonstrated a new source that integrates a 213 nm laser allowing for a ~3 μm footprint using front-side laser optics.[53] Alternatively, Zavalin and coworkers developed a transmission-mode geometry MALDI source, where the UV-laser is redirected to ablate the sample from the back side. By decoupling the laser and ion optics, higher numerical aperture objectives can be utilized without impeding the ion path, resulting in ~1 μm spot sizes.[54] However, a drawback of any high spatial resolution IMS experiment is a reduction in ion abundances; the Caprioli[55] and Dreisewerd[47] laboratories incorporated a secondary laser perpendicular to the primary ablation plume as a means to enhance ionization of transmission geometry setups. An example of these data sets is featured here (Figure 1A).

2.2. Secondary Ion Mass Spectrometry.

SIMS utilizes electrostatically focused primary ions (e.g., Bi^+, Cs^+, and O^-) or clusters (e.g., Au_3^+, C_{60}, and Ar) to impact the sample surface, causing a collisional cascade in the top few monolayers of the sample leading to the ejection of secondary ions.[2,34] Because of the high energy of the ion beam, analyte ions often undergo significant fragmentation and analysis is typically limited to molecular weight ions <2 kDa.[56] The energy of the ion beam plays a critical role in sampling and can be divided into two regimes: static and dynamic SIMS. Static SIMS is defined by low primary ion doses ($<10^{13}$ cm^{-2}) and beam currents (pA-nA) suitable for surface analysis of elements and molecules. Alternatively, dynamic SIMS has much higher primary ion doses ($>10^{13}$ cm^{-2}) and beam currents (mA), making it suitable for depth profiling and three-dimensional imaging.[57] In general, sample preparation for SIMS analysis is minimal and consists of mounting tissues flatly onto conductive targets and drying prior to introduction into the source vacuum chamber.[58,59] Although not required, washing samples to remove salts from tissue prior to analysis can improve ion yield.[60,61]

The primary advantage of SIMS is its high spatial resolution capabilities because ion beams can be tightly focused using electric fields (1 μm to 30 nm).[32] Similar to MALDI, SIMS spatial resolution is defined by the diameter of the ion beam at the surface and the pitch. SIMS has been used for cellular and subcellular analyses[62–65] and for the determination of molecular profiles of various disorders, including different cancer types[66] and cardiovascular disease.[67] It has also been used to monitor signaling between bacterial cocultures and distinct alkyl quinolone messengers between different strains of *Pseudomonas aeruginosa* (Figure 1B).[48] Additionally, SIMS was employed to visualize salt redistribution in brain tissue between healthy and stroke mice.[68] While effective for low molecular weight metabolite and lipid analyses, it has not been commonly applied to peptide and protein imaging studies.

2.3. Desorption Electrospray Ionization.

DESI is performed by spraying charged solvent droplets on the surface of the sample where the analytes are desorbed and ionized for subsequent detection by MS.[69] The imaging experiment is performed in a continuous raster sampling mode where the target is moved continuously under the DESI spray in a “typwriter-like” motion. Spatial resolution is estimated by the target stage velocity, sampling rate of the mass spectrometer, number of spectra averaged for a single pixel, and distance between adjacent line scans. Although DESI has limited spatial resolution capabilities (~150 μm), it requires minimal to no sample preparation. Tissues sections are mounted onto glass slides and sampling is performed at ambient pressure. Recently, the Laskin lab developed a modified form of this sampling approach, termed nanoDESI, using a liquid microjunction to increase spatial resolution to ~10 μm (Figure 1C).[49] While nanoDESI is not discussed in a multimodal imaging context here, we eagerly anticipate the higher spatial resolution of nanoDESI being coupled to other modalities. Moreover, DESI and nanoDESI been used to map metabolite,[70–72] lipid,[73–76] and drug distributions in a variety of biological systems ranging from plants to diseased mammalian tissue.[77–79] Further, additives in DESI solvent can target specific molecules in the case of reactive DESI[80] or enhance extraction.[70]

DESI and nanoDESI IMS are minimally destructive techniques and have been used experimentally in surgical settings to enable intraoperative molecular assessment and aid in real-time intraoperative decisions.[36,81,82] Sans et al. molecularly characterized high-grade serous carcinoma, serous borderline ovarian tumors and normal ovarian tissue samples using DESI IMS.[83] They identified predictive markers of cancer aggressiveness and built classification models to enable diagnosis and prediction of high-grade serous carcinoma in comparison to normal tissue with a high certainty of ~96%. Similar work from the Eberlin lab has led to the development of a hand-held mass spectrometry device, the MasSpec Pen, which enables *in vivo* diagnostics during surgery.[84–86] This device has been used for classifying ovarian[87] and breast cancer[88] since it was originally developed. Because it can be operated at atmospheric pressure and requires minimal sample preparation, DESI holds promise for use in clinical and surgical settings.

3. COMBINING MULTIPLE IMAGING MASS SPECTROMETRY TECHNOLOGIES

Because each IMS technology has unique performance characteristics for different molecular classes, there is utility in coupling them together. Technologies such as tandem MS, microextractions, and ion mobility each add additional dimensions to the MS data set, expanding upon the chemical information that can be obtained, either by enabling *de novo* identification or reducing spectral complexity.

3.1. Spatially Targeted Tandem MS.

Tandem mass spectrometry enables *de novo* identification of molecules within complex samples.[89–91] Tandem MS is generally accomplished by performing isolation within one mass analyzer for subsequent fragmentation and transmittance into another mass analyzer for detection.[92] Serially performing these analyses allows for identification of discrete molecules within a biological sample.[93,94] In the context of imaging, pixels can be subdivided allowing for a precursor ion scan and subsequent MS/MS scans. This spatially targeted structural information comes at the cost of spatial resolution to accommodate multiple samplings. Additionally, it is often difficult to perform tandem MS analysis within an imaging experiment if the ion of interest is only present within a small number of disperse features or pixels.[17] Alternative means of targeting sample regions or locations for identifying key ions include multimodal image-guided surface sampling,[95,96] microprobe extraction for offline tandem MS,[97–99] and tandem MS on an orthogonal sample.[16,30] By using these various strategies, ions that are found in a small number of pixels or structural features can be targeted for analysis.

Tandem MS can be used within an imaging context to identify the differential localization of isomers or isobars within a tissue. Although tandem MS has been reported for several types of IMS technologies,[100–102] it is primarily used for SIMS imaging because most ion beams fragment analyte ions during the ionization process.[103–107] Any imaging mass spectrometer with MS/MS capabilities can generate fragment ion images[108,109] enabling direct visualization and differentiation of isomers and isobars within tissue without prior

separation or derivatization. Generally, these experiments are usually limited to surveying a small number of ions within a sample, since the tissue is partially consumed during analysis.

3.2. Multi-Imaging Mass Spectrometry Experiments.

Each of the three types of IMS technologies discussed here provide different molecular coverage and spatial resolution. As a result, investigators have combined some of these to gain further functionality. SIMS and MALDI IMS have been combined to detect multiple chemical classes, such as low molecular weight metabolites and lipids within individual cells[95] and tissue.[111] Additionally, the combination of MALDI and SIMS has been used to analyze hair to enhance sensitivity and spatial resolution.[112,113] Both MALDI and SIMS sources are operated under vacuum using similar tissue preparation protocols. In some cases, SIMS analyses have been shown to be enhanced by the application of a MALDI matrix.[114,115] While less common, combining MALDI and DESI together enables analysis of different lipid species[116] and comapping of lipids and proteins.[117] To our knowledge, there has not yet been a DESI and SIMS multimodal IMS experiment, likely because of the differences in sample preparation. Reaction additives can be employed for DESI analyses for quantitation and derivatization chemistries, bringing additional capabilities to any combination of technologies. Finally, DESI produces multiply charged ions that are often more amenable to tandem MS applications.

3.3. Microextraction.

Microextraction protocols aim to remove key analytes from bulk material to reduce chemical complexity[118] and target specific analytes. Both solid and liquid phase extraction techniques have been coupled to IMS for increased peak capacity and sensitivity. Solid phase microextraction (SPME) comprises a diverse set of solventless techniques that allow for *in vivo* analysis. An advantage of SPME devices is that most analytes are introduced into the MS system at once. Introducing ions concurrently increases sensitivity and signal-to-noise (S/N) compared to technologies that generate a transient signal.[119,120] Furthermore, SPME is used to separate an analyte of interest from bulk material, such as in trace analyte analysis.[121]

Liquid extractions, such as liquid microjunction (LMJ)[96,122]and liquid extraction surface analysis (LESA),[97,123] also enhance peak capacity and reduce ion suppression. Briefly, extraction solvents are dispensed onto a tissue surface and collected for subsequent liquid chromatography or capillary electrophoresis MS analysis.[50] Spatially targeted liquid extractions are advantageous because they can be coupled to different separation techniques, increasing both sensitivity and depth of coverage. For instance, Cahill et al. used an LMJ extraction to image portions of a microfluidic device while it was functioning with future use aimed at biology-based microfluidic devices.[124] Typically, this technology utilizes relatively large areas for droplet placement. However, recently microLESA was combined with piezoelectric spotting of trypsin to achieve higher spatial resolution sampling than previously reported.[97,125] In addition, microLESA was integrated with autofluorescence microscopy to correlate protein signatures of murine kidney and *Staphylococcus aureus* abscesses without tissue staining.[97] As these techniques continue to improve in spatial resolution and automated platforms become available, combining IMS with spatially

targeted microextractions will be adapted to supplement spatial information with deeper molecular coverage and added identification capabilities.

3.4. Ion Mobility.

Ion mobility separations add an orthogonal analytical dimension to IMS that reduces ion interference for improving peak capacity and specificity and aiding in identification of species. Additionally, drift time or collision cross sections (CCS) calculated with the use of standards can be used to help identify isomers and isobars. Ion mobility techniques that have been coupled to IMS include drift tube mass spectrometry (DTIMS),[126,127] traveling wave ion mobility spectrometry (TWIMS),[128,129] field asymmetric ion mobility spectrometry (FAIMS)[130–132] and, more recently, trapped ion mobility spectrometry (TIMS).[133–135]

A major focus of the ion mobility field is developing higher resolving power platforms, so they can separate isomers and isobars. Park, Fernandez-Lima, and coworkers utilized a buffer gas and ion trapping by electric field gradient for the development of TIMS devices. They report resolving powers of ~200 but up to ~400.[136–138] One approach for increasing resolution is by increasing path length and/or number of passes around the mobility device. Notable ion mobility advancements include the development of structures for lossless ion manipulation (SLIM) devices,[139,140] as well as the cyclic ion mobility (cIM).[141] SLIM devices utilize a separation path length of ~540 m[142] for achieving resolving powers over 1800. Using cIM, resolving power of 750 (with 100 passes) has been reported using a reverse sequence peptide pair. Although, sensitivity can be challenging in these devices as ions are lost radially over time. Recently cIM has been integrated with LESA for the improvement of S/N and the number of detected proteins from tissue samples (Figure 2).[110]

Beyond increasing peak capacity and specificity, trendlines within ion mobility heat maps can be used to identify different molecular species, classes, and subclasses.[143] For example, MALDI DTIMS IMS was used successfully to separately image a lipid species ([phosphatidylcholine(34:2)+H]$^+$) from a closely isobaric peptide ion (RPPGFSP).[144] Škrášková et al. visualized multiply charged polysialylated gangliosides using DESI TWIMS.[116] Recently TIMS has been integrated with MALDI IMS to the separate and map isobaric lipid species directly from tissue.[145] Cooper and coworkers introduced a new cylindrical FAIMS device coupled to LESA IMS. This workflow improved the number of detected proteins from what was previously reported as much as 10 times in murine brain, testes, and kidney.[146] Clearly, ion mobility has great potential for IMS applications as it provides the ability to overcome the analytical challenges associated with direct sampling of complex biological tissues. Software is continually being developed to more efficiently process highly dimensional ion mobility IMS data.

4. INTEGRATION WITH OTHER TECHNOLOGIES

Non-MS analytical technologies can be integrated with MS technologies to increase chemical coverage. Since each technology has distinctive advantages for different molecular classes, experiments that synergistically incorporate multiple technologies gain unique chemical information neither one can obtain alone. For example, many cell types and functional cell states are uniquely suited for analysis by specific methods, such as

transcriptomics or immunostaining, and integrating these can add great utility to the molecular specificity of MS.

4.1. Microscopy.

Microscopy is one of the oldest analytical approaches dating back to the early 17th century and is commonly applied to biological and clinical problems.[148–151] Overall, microscopy images are generated by capturing electromagnetic radiation or particle beams as they interact with the sample through reflection, refraction, or diffraction. A series of lenses and objectives focus the light/particles enabling imaging with high magnification.

Brightfield and histological stains, such as hematoxylin and eosin (H&E) and periodic acid-Schiff (PAS), are used extensively in pathology to assess tissue integrity, health, and disease.[152–154] Stained tissues have been employed with IMS to connect molecular profiles to histological features of both healthy and diseased tissue, such as cancer[155–159] and functional disorders.[160,161] Recently, Basu et al. enabled IMS and histology to be rapidly correlated by incorporating matrix precoated slides, templates, and a 10 kHz laser.[162] Histological stains are ubiquitous within the scientific and medical field, so multimodal studies that combine IMS and stained microscopy improve interpretation and facilitate collaboration between the technologists and the biologists or physicians. Similarly, simple brightfield images can be used for correlation of IMS signals to specific tissue structures, particularly in cases that have features that are easily distinguished with brightfield microscopy.[163,164]

Fluorescence microscopy of both endogenous fluorophores[165,166] and tagged antibodies[167–169] or nucleic acids[170,171] have also been fundamental to our understanding of biological systems. For example, Vardi et al. used autofluorescence from chlorophyll and MALDI IMS to study lipid metabolism within algal plaques.[172] By targeting key proteins or genes, investigators can parse metabolic pathways and monitor how these change as a function of disease state or demographic. While exceptionally powerful and informative, these technologies are generally limited to studying peptides or proteins since there are few probes available for low molecular weight metabolites and lipids.[173,174] IMS has been readily coupled to fluorescence microscopy approaches to tie together cell-type specific immune[16,17,175,176] and transcript profiles[177–179] to metabolites detected by IMS.[180] Immunohistochemistry can be used to histologically classify and contextualize the chemical information obtained by IMS. Moreover, the combination of both IMS and immunohistochemistry produce more rigorous classification schemes than either modality independently. Recently, several laboratories have combined immunohistochemistry and IMS to correlate protein or metabolite signals to specific tissue substructures.[181–184] This type of experiment is further extended by recent work where investigators coupled multiplexed immunohistochemistry with MALDI FT-ICR IMS to determine metabolic profiles of cancer cells, incorporating molecular classes.[185] The increase in the plexity of the immunofluorescence labels additionally enhances the specificity of chemical profiles created by MS analysis, as these immunofluorescence labels can be correlated to more specific tissue regions or cell types.

Immunofluorescence imaging has been correlated with MALDI IMS[176] and fluorescence in situ hybridization (FISH) with SIMS.[177] We could not find an example of either being used as part of DESI multimodal studies. This is interesting because there are no experimental considerations preventing IHC or FISH from being combined with all the IMS modalities discussed here. However, technical challenges in coregistering modalities with dramatic differences in spatial resolution may be driving this perceived disparity. Patterson et al. have developed combination experimental and computational pipelines using autofluorescence microscopy to overcome this challenge for multimodal MALDI IMS studies.[165,166] It is anticipated that fluorescence microscopy will become an important correlative technology in IMS studies.

Particle-based microscopy, such as scanning electron microscopy (SEM) and transmission electron microscopy (TEM), offer very high spatial resolution because it is not diffraction limited. A series of ion optics are used to focus ions toward a sample. The ions then interact with the sample and the emerging electrons and various energy conversion products (e.g., secondary electrons, X-rays, light) are captured as an image. Because nanoSIMS and electron microscopies have similar sample and operational requirements, they have often been used on the same sample.[187] TOF-SIMS has been integrated into a helium ion microscope for 8 nm imaging with the potential for extremely high resolution molecular imaging of biological samples (Figure 3).[147] For example, nanoSIMS and TEM have been combined to map dopamine distributions in dense core vesicles, providing key insight into vesicle loading and nanocompartmentalization.[188] Another study involves integration of fluorescence microscopy, SIMS, high-energy resolution X-ray photoelectron spectroscopy, and SEM on the same plant root to study bacterial growth and infection on this root.[189] The authors combined these four modalities because of the simple and compatible sample preparation involved for each. Beyond registration for enhanced localization, particle-based microscopy is also readily used to assess MALDI matrix application for ensuring matrix coverage and crystal size.[190,191]

4.2. Spectroscopy.

Spectroscopic imaging includes a suite of optical approaches, such as infrared (IR)[192] and Raman, that provide unique spectra of complex chemical mixtures, creating reproducible chemical profiles of different physiological regions and disease states.[193] Spectroscopy is used in a wide array of biological studies[194–199] because the approaches are generally nondestructive, label-free, and capable of high spatial resolutions (diffraction limited, 250 nm). While each spectroscopic approach activates different, well characterized molecular modes, it is often difficult to correlate spectroscopic signatures of complex mixtures to discrete chemicals. Rather, they provide general information on bond types and functional groups for the entire chemical mixture.[200–203] As such, spectroscopy has been coupled to a variety of MS technologies, including IMS, to provide more detailed molecular descriptions of samples.[204–206] Because spectroscopic analysis is label-free and nondestructive, both modalities can be performed on the same tissue section.[207]

Raman and IMS have been correlated to study bacteria,[208–210] plants,[211] single cells,[212] and mammalian organs.[213,214] Fourier transform infrared microscopy (FT-IR) has similarly

been coupled to IMS for many biological studies.[207,215,216] Recently, Rabe et al. developed a method for FT-IR guided MALDI IMS (Figure 4). By coupling these two technologies together, the authors reduced data load and acquisition time by >90%.[186] Magnetic resonance imaging has also been used to compliment molecular specificity of IMS with dynamic, whole organ imaging.[217–222] While MALDI IMS has primarily been coupled to spectroscopic measurements, we foresee DESI increasingly becoming incorporated with Raman and magnetic resonance imaging. DESI does not have many tissue preparation requirements and can theoretically be directly integrated within either approach. Moreover, Raman and magnetic resonance spectra are not saturated when water is present, unlike IR, which readily is absorbed by water, making them ideal candidates for multimodal DESI experiments.

4.3. Transcriptomics.

Transcriptomics technologies measure gene expression through the extraction and amplification of nucleic acids, most generally ribonucleic acids.[223–225] Because of the exponential amplification that can occur, this group of technologies is highly sensitive and has been the driving force behind cell typing and classification. There is great interest in coupling IMS with transcriptomics analysis as it would enable simultaneous correlation of gene expression to gene products and biproducts. A majority of the literature combining mass spectrometry and transcriptomics measurements has involved liquid chromatography for bulk proteomics and/or metabolomics.[226,227] Toward an imaging context, investigators probed an insect, *Carausius morosus*, for neuropeptide content with MALDI MS and correlated this to bulk sequencing to uncover peptides with no known homology.[228] Although this was not an imaging application, the sample preparation was performed in such a way that this workflow could be adapted to an imaging workflow. As an additional step toward combining IMS with transcriptomics, the Knepper et al. microdissected kidney tubules and performed RNA-seq and proteomics.[229] This methodology incorporates spatial information on the microdissected structures, which is an important step toward coupling IMS and transcriptomics directly. Moreover, there has been some exciting work where transcriptomics and proteomics IMS information has been correlated on different bulk samples.[230] Work combining two approaches on the same sample provided insight into the link between fatty acids and immunity within breast cancer[231] and role of liver X receptors in male reproduction.[232] While only a few examples exist, the combination of transcriptomics and IMS will continue to increase in the coming years and has the potential to uncover new connections that span the central dogma of molecular biology.

4.4. Electrochemistry.

Electrochemistry has been vital in the study of electroactive signaling molecules, such as dopamine, epinephrine, serotonin, and histamine within biological systems.[233–235] This is partly because it is capable of absolute quantitation of femto- to zeptomole amounts of analyte at μs temporal resolutions. It is highly selective and naturally applicable to the analysis of many low molecular weight metabolites, such as neurotransmitters.[236] nanoSIMS/nanoSIMS and electrochemistry are compatible and have been used together often to study nonbiological[237] and biological samples alike.[236,238,239] Ewing et al. have quantitated L-DOPA concentrations in vesicles and other organelles using nanoSIMS

and validated these concentrations with electrochemistry.[240] This is particularly important because it enables quantitation of low molecular weight metabolites at high spatial resolutions. Further, Larsson and coworkers quantitated octopamine release during different stimulations using nanoSIMS and an embedded electrode.[241] Investigators in the IMS field have also adapted many technologies and developments from electrochemical studies,[242] ranging from nanopipettes to electrochemical principals of ion generation. Adopting materials, analyses, or processes from other fields is an effective, time saving process that expedites scientific advancements.

5. FUTURE OF THE FIELD

Mass spectrometry technologies have rapidly advanced with improved sampling, ion transmission, and detector sensitivity, enabling highly sensitive and specific analysis of biological tissues. Under favorable conditions, MS can detect concentrations as low as 10 zeptomoles or approximately 6000 molecules.[6] This sensitivity is sufficient for probing most molecules within biological systems and yet there is still much we do not understand. Nevertheless, improvements in the molecular, spatial, temporal, and biological specificity are required to answer remaining questions. IMS is one available tool that provides untargeted, highly multiplexed molecular analysis, but only through the combination with other technologies can we achieve specificity in all these areas mentioned above. Multimodal imaging experiments can significantly improve performance characteristics, including structural identification, throughput, cell type specificity, and dynamic range of MS-based chemical profiles. The present article has summarized the current literature surrounding multimodal IMS and the development of the field to further explore remaining biological questions.

A major task facing multimodal approaches involves efforts to fully integrate the several data sets to enable deeper data mining. This is particularly difficult within an imaging regime because the various technologies can have dramatically different spatial resolutions, data structures, and chemical information. Different computation methods for addressing differences within spatial resolution include various methods of up sampling the data, performing more refined data fusion, as well as other experimental approaches.[165,166,243–246] While these are capable of connecting modalities that are similar in resolution, significant experimental and technological capabilities are required to avoid the introduction of artifacts.[207] While many imaging modalities are within an order of magnitude of one another, this will influence the capacity to combine lower spatial resolution IMS technologies like DESI with higher resolution molecular imaging approaches, like SEM.

Moreover, technologies provide both overlapping and orthogonal information that is often difficult to correlate. For instance, transcriptomics measures gene expression of different biochemical pathways that result with peptide and metabolomic products. Ideally, a highly expressed gene would indicate the presence of a specific metabolite and IMS would detect this same metabolite in high abundance within the same regions, but this is not always the case. There many transport, degradation, and modification pathways that impede this correlation and create complex data sets that are difficult to interpret. Additional

compounding technical factors, such as matrix effects, differences in ionization efficiencies, and limited dynamic range add to this complexity. While transcriptomics is used as an example here, a similar scenario applies to other multimodal approaches, such as protein abundances between IMS and immunofluorescence experiments or lipid analysis by Raman spectroscopy and IMS. While challenging, future multimodal experiments will slowly begin to unravel the complex relationships between the data produced by orthogonal technologies. In connection with this, new machine learning algorithms and approaches will be essential for untangling the abundance of chemical information obtained with multimodal IMS. This will inevitably lead to a more complete picture of biological systems and pathways.

Finally, improving sample preparation and workflows will undoubtedly improve the quality and reproducibility of collected data, particularly as these technologies enter the rigorous domain of medicine and clinical trials. Many technologies cannot be combined “out of the box”, and so there are often trade-offs made to enable multimodal analysis. Although, the gained information from the suboptimal combination of the approaches is often greater than the data of either technique alone. Developing methods that enable multiple imaging modalities to be performed optimally and with minimal spatial compromise will dramatically improve the ability to integrate and discover connections between multimodal data sets. Optimizing the ways and methods behind combining the different approaches is a clear path forward in the field.

In summary, multimodal IMS is a remarkably diverse endeavor that incorporates the best attributes from a variety of scientific disciplines. In the future, multimodal IMS technologies will progressively become more common as the scientific community begins to study more complex biological and medicinal questions. Such studies have the potential to bring together genomic, proteomic, and metabolomic imaging technologies to provide unprecedented insights into biology and medicine.

ACKNOWLEDGMENTS

Support was provided by the NIH Common Fund and National Institute of Diabetes and Digestive and Kidney Diseases (Grant U54DK120058 awarded to J.M.S. and R.M.C.), NIH National Institute of Allergy and Infectious Disease (Grant R01 AI138581 awarded to J.M.S.), the National Science Foundation Major Research Instrument Program (Grant CBET-1828299 awarded to J.M.S. and R.M.C.), and by the NIH National Institute of General Medical Sciences (Grant 2P41GM103391 awarded to R.M.C.). E.K.N. is supported by a National Institute of Environmental Health Sciences training grant (T32ES007028).

REFERENCES

(1). Bodzon-Kulakowska A; Suder P Imaging mass spectrometry: Instrumentation, applications, and combination with other visualization techniques. Mass Spectrom. Rev 2016, 35, 147. [PubMed: 25962625]

(2). Xu X; Zhong J; Su Y; Zou Z; He Y; Hou X A brief review on mass/optical spectrometry for imaging analysis of biological samples. Appl. Spectrosc. Rev 2019, 54, 57.

(3). Ho Y-N; Shu L-J; Yang Y-L Imaging mass spectrometry for metabolites: technical progress, multimodal imaging, and biological interactions. WIREs Systems Biology and Medicine 2017, 9, e1387.

(4). Buchberger AR; DeLaney K; Johnson J; Li L Mass Spectrometry Imaging: A Review of Emerging Advancements and Future Insights. Anal. Chem 2018, 90, 240. [PubMed: 29155564]

(5). Xu G; Li J Recent advances in mass spectrometry imaging for multiomics application in neurology. J. Comp. Neurol 2019, 527, 2158. [PubMed: 30393860]

(6). Neumann EK; Do TD; Comi TJ; Sweedler JV Exploring the Fundamental Structures of Life: Non-Targeted, Chemical Analysis of Single Cells and Subcellular Structures. Angew. Chem., Int. Ed 2019, 58, 9348.

(7). LEón M; Ferreira CR; Eberlin LS; Jarmusch AK; Pirro V; Rodrigues ACB; Favaron PO; Miglino MA; Cooks RG Metabolites and Lipids Associated with Fetal Swine Anatomy via Desorption Electrospray Ionization – Mass Spectrometry Imaging. Sci. Rep 2019, 9, 7247. [PubMed: 31076607]

(8). Bergman H-M; Lindfors L; Palm F; Kihlberg J; Lanekoff I Metabolite aberrations in early diabetes detected in rat kidney using mass spectrometry imaging. Anal. Bioanal. Chem 2019, 411, 2809. [PubMed: 30895347]

(9). Morse N; Jamaspishvili T; Simon D; Patel PG; Ren KYM; Wang J; Oleschuk R; Kaufmann M; Gooding RJ; Berman DM Reliable identification of prostate cancer using mass spectrometry metabolomic imaging in needle core biopsies. Lab. Invest 2019, 99, 1561. [PubMed: 31160688]

(10). Wang M; Dubiak K; Zhang Z; Huber PW; Chen DDY; Dovichi NJ MALDI-imaging of early stage Xenopus laevis embryos. Talanta 2019, 204, 138. [PubMed: 31357275]

(11). Shariatgorji M; Nilsson A; Fridjonsdottir E; Vallianatou T; Källback P; Katan L; Sävmarker J; Mantas I; Zhang X; Bezard E; Svenningsson P; Odell LR; Andrén PE Comprehensive mapping of neurotransmitter networks by MALDI–MS imaging. Nat. Methods 2019, 16, 1021. [PubMed: 31548706]

(12). Watrous JD; Dorrestein PC Imaging mass spectrometry in microbiology. Nat. Rev. Microbiol 2011, 9, 683. [PubMed: 21822293]

(13). Shank EA; Kolter R Extracellular signaling and multi-cellularity in Bacillus subtilis. Curr. Opin. Microbiol 2011, 14, 741. [PubMed: 22024380]

(14). Alamri H; Patterson NH; Yang E; Zoroquiain P; Lazaris A; Chaurand P; Metrakos P Mapping the triglyceride distribution in NAFLD human liver by MALDI imaging mass spectrometry reveals molecular differences in micro and macro steatosis. Anal. Bioanal. Chem 2019, 411, 885. [PubMed: 30515538]

(15). Sämfors S; Fletcher JS Lipid Diversity in Cells and Tissue Using Imaging SIMS. Annu. Rev. Anal. Chem 2020, 13, 249.

(16). Neumann EK; Comi TJ; Rubakhin SS; Sweedler JV Lipid Heterogeneity between Astrocytes and Neurons Revealed by Single-Cell MALDI-MS Combined with Immunocytochemical Classification. Angew. Chem., Int. Ed 2019, 58, 5910.

(17). Neumann EK; Ellis JF; Triplett AE; Rubakhin SS; Sweedler JV Lipid Analysis of 30 000 Individual Rodent Cerebellar Cells Using High-Resolution Mass Spectrometry. Anal. Chem 2019, 91, 7871. [PubMed: 31122012]

(18). Nemes P; Woods AS; Vertes A Simultaneous Imaging of Small Metabolites and Lipids in Rat Brain Tissues at Atmospheric Pressure by Laser Ablation Electrospray Ionization Mass Spectrometry. Anal. Chem 2010, 82, 982. [PubMed: 20050678]

(19). Eberlin LS; Dill AL; Golby AJ; Ligon KL; Wiseman JM; Cooks RG; Agar NYR Discrimination of Human Astrocytoma Subtypes by Lipid Analysis Using Desorption Electrospray Ionization Imaging Mass Spectrometry. Angew. Chem., Int. Ed 2010, 49, 5953.

(20). Angel PM; Spraggins JM; Baldwin HS; Caprioli R Enhanced sensitivity for high spatial resolution lipid analysis by negative ion mode matrix assisted laser desorption ionization imaging mass spectrometry. Anal. Chem 2012, 84, 1557. [PubMed: 22243218]

(21). Brunelle A; Laprévote O Lipid imaging with cluster time-of-flight secondary ion mass spectrometry. Anal. Bioanal. Chem 2009, 393, 31. [PubMed: 18777109]

(22). Rešetar Maslov D; Svirkova A; Allmaier G; Marchetti-Deschamann M; Kraljevicć Pavelicć S Optimization of MALDI-TOF mass spectrometry imaging for the visualization and comparison of peptide distributions in dry-cured ham muscle fibers. Food Chem 2019, 283, 275. [PubMed: 30722871]

(23). Do TD; Ellis JF; Neumann EK; Comi TJ; Tillmaand EG; Lenhart AE; Rubakhin SS; Sweedler JV Optically Guided Single Cell Mass Spectrometry of Rat Dorsal Root Ganglia to Profile Lipids, Peptides and Proteins. ChemPhysChem 2018, 19, 1180. [PubMed: 29544029]

(24). Caprioli RM; Farmer TB; Gile J Molecular Imaging of Biological Samples: Localization of Peptides and Proteins Using MALDI-TOF MS. Anal. Chem 1997, 69, 4751. [PubMed: 9406525]

(25). Dilillo M; Ait-Belkacem R; Esteve C; Pellegrini D; Nicolardi S; Costa M; Vannini E; Graaf E. L. d.; Caleo M; McDonnell LA Ultra-High Mass Resolution MALDI Imaging Mass Spectrometry of Proteins and Metabolites in a Mouse Model of Glioblastoma. Sci. Rep 2017, 7, 603. [PubMed: 28377615]

(26). Garza KY; Feider CL; Klein DR; Rosenberg JA; Brodbelt JS; Eberlin LS Desorption Electrospray Ionization Mass Spectrometry Imaging of Proteins Directly from Biological Tissue Sections. Anal. Chem 2018, 90, 7785. [PubMed: 29800516]

(27). Andersson M; Groseclose MR; Deutch AY; Caprioli RM Imaging mass spectrometry of proteins and peptides: 3D volume reconstruction. Nat. Methods 2008, 5, 101. [PubMed: 18165806]

(28). Groseclose MR; Andersson M; Hardesty WM; Caprioli RM Identification of proteins directly from tissue: in situ tryptic digestions coupled with imaging mass spectrometry. J. Mass Spectrom 2007, 42, 254. [PubMed: 17230433]

(29). Crecelius AC; Cornett DS; Caprioli RM; Williams B; Dawant BM; Bodenheimer B Three-dimensional visualization of protein expression in mouse brain structures using imaging mass spectrometry. J. Am. Soc. Mass Spectrom 2005, 16, 1093. [PubMed: 15923124]

(30). Ryan DJ; Spraggins JM; Caprioli RM Protein identification strategies in MALDI imaging mass spectrometry: a brief review. Curr. Opin. Chem. Biol 2019, 48, 64. [PubMed: 30476689]

(31). Angeletti S; Ciccozzi M Matrix-assisted laser desorption ionization time-of-flight mass spectrometry in clinical microbiology: An updating review. Infect., Genet. Evol 2019, 76, 104063. [PubMed: 31618693]

(32). Eswara S; Pshenova A; Yedra L; Hoang QH; Lovric J; Philipp P; Wirtz T Correlative microscopy combining transmission electron microscopy and secondary ion mass spectrometry: A general review on the state-of-the-art, recent developments, and prospects. Appl. Phys. Rev 2019, 6, 021312.

(33). Gyngard F; Steinhauser ML Biological explorations with nanoscale secondary ion mass spectrometry. J. Anal. At. Spectrom 2019, 34, 1534. [PubMed: 34054180]

(34). Gao D; Huang X; Tao Y A critical review of NanoSIMS in analysis of microbial metabolic activities at single-cell level. Crit. Rev. Biotechnol 2016, 36, 884. [PubMed: 26177334]

(35). Zheng Q; Chen H Development and Applications of Liquid Sample Desorption Electrospray Ionization Mass Spectrometry. Annu. Rev. Anal. Chem 2016, 9, 411.

(36). Ferreira C; Alfaro CM; Pirro V; Cooks RG Desorption Electrospray Ionization Mass Spectrometry Imaging: Recent Developments and Perspectives. J. Biomol Tech 2019, 30, S46.

(37). Javanshad R; Venter AR Ambient ionization mass spectrometry: real-time, proximal sample processing and ionization. Anal. Methods 2017, 9, 4896.

(38). Parrot D; Papazian S; Foil D; Tasdemir D Imaging the Unimaginable: Desorption Electrospray Ionization – Imaging Mass Spectrometry (DESI-IMS) in Natural Product Research. Planta Med 2018, 84, 584. [PubMed: 29388184]

(39). Shrestha B; Walsh CM; Boyce GR; Nemes P In Advances in MALDI and Laser-Induced Soft Ionization Mass Spectrometry; Springer: 2016; p 149.

(40). Dunham SJB; Neumann EK; Lanni EJ; Ong T-H; Sweedler JV Biomarker Discovery with Mass Spectrometry Imaging and Profiling. In Proteomics for Biological Discovery; John Wiley & Sons: 2019; p 89–123.

(41). Strupat K; Karas M; Hillenkamp F 2,5-Dihydroxybenzoic acid: a new matrix for laser desorption—ionization mass spectrometry. Int. J. Mass Spectrom. Ion Processes 1991, 111, 89.

(42). Beavis RC; Chaudhary T; Chait BT α-Cyano-4-hydroxycinnamic acid as a matrix for matrixassisted laser desorption mass spectromtry. Org. Mass Spectrom 1992, 27, 156.

(43). Vermillion-Salsbury RL; Hercules DM 9-Aminoacridine as a matrix for negative mode matrix-assisted laser desorption/ionization. Rapid Commun. Mass Spectrom 2002, 16, 1575.

(44). Korte AR; Lee YJ MALDI-MS analysis and imaging of small molecule metabolites with 1,5-diaminonaphthalene (DAN). J. Mass Spectrom 2014, 49, 737. [PubMed: 25044901]

(45). Scott AJ; Flinders B; Cappell J; Liang T; Pelc RS; Tran B; Kilgour DPA; Heeren RMA; Goodlett DR; Ernst RK Norharmane matrix enhances detection of endotoxin by MALDI-MS for simultaneous profiling of pathogen, host and vector systems. Pathog. Dis 2016, 74. DOI: 10.1093/femspd/ftw097

(46). Amstalden van Hove ER; Smith DF; Heeren RMA A concise review of mass spectrometry imaging. Journal of Chromatography A 2010, 1217, 3946. [PubMed: 20223463]

(47). Niehaus M; Soltwisch J; Belov ME; Dreisewerd K Transmission-mode MALDI-2 mass spectrometry imaging of cells and tissues at subcellular resolution. Nat. Methods 2019, 16, 925. [PubMed: 31451764]

(48). Cao T; Morales-Soto N; Jia J; Baig N; Dunham SJ; Ellis J; Sweedler J; Shrout J; Bohn P Spatiotemporal dynamics of molecular messaging in bacterial co-cultures studied by multimodal chemical imaging; SPIE, 2019; Vol. 10863.

(49). Yin R; Burnum-Johnson KE; Sun X; Dey SK; Laskin J High spatial resolution imaging of biological tissues using nanospray desorption electrospray ionization mass spectrometry. Nat. Protoc 2019, 14, 3445. [PubMed: 31723300]

(50). Boughton BA; Thinagaran D; Sarabia D; Bacic A; Roessner U Mass spectrometry imaging for plant biology: a review. Phytochem. Rev 2016, 15, 445. [PubMed: 27340381]

(51). Trim PJ; Snel MF Small molecule MALDI MS imaging: Current technologies and future challenges. Methods 2016, 104, 127. [PubMed: 26804564]

(52). Murray KK; Seneviratne CA; Ghorai S High resolution laser mass spectrometry bioimaging. Methods 2016, 104, 118. [PubMed: 26972785]

(53). Heiles S; Kompauer M; Müller MA; Spengler B Atmospheric-Pressure MALDI Mass Spectrometry Imaging at 213 nm Laser Wavelength. J. Am. Soc. Mass Spectrom 2020, 31, 326. [PubMed: 32031384]

(54). Zavalin A; Yang J; Hayden K; Vestal M; Caprioli RM Tissue protein imaging at 1 μm laser spot diameter for high spatial resolution and high imaging speed using transmission geometry MALDI TOF MS. Anal. Bioanal. Chem 2015, 407, 2337. [PubMed: 25673247]

(55). Spivey EC; McMillen JC; Ryan DJ; Spraggins JM; Caprioli RM Combining MALDI-2 and transmission geometry laser optics to achieve high sensitivity for ultra-high spatial resolution surface analysis. J. Mass Spectrom 2019, 54, 366. [PubMed: 30675932]

(56). Wogelred L; Höök F; Agnarsson B; Sjövall P Toward multiplexed quantification of biomolecules on surfaces using time-of-flight secondary ion mass spectrometry. Biointerphases 2018, 13, 03B413.

(57). Sodhi RNS Time-of-flight secondary ion mass spectrometry (TOF-SIMS):—versatility in chemical and imaging surface analysis. Analyst 2004, 129, 483. [PubMed: 15152322]

(58). Yoon S; Lee TG Biological tissue sample preparation for time-of-flight secondary ion mass spectrometry (ToF–SIMS) imaging. Nano Convergence 2018, 5, 24. [PubMed: 30467706]

(59). Schaepe K; Jungnickel H; Heinrich T; Tentschert J; Luch A; Unger WES In Characterization of Nanoparticles; Hodoroaba V-D, Unger WES, Shard AG, Eds.; Elsevier: 2020; p 481.

(60). Gilmore IS; Heiles S; Pieterse CL Metabolic Imaging at the Single-Cell Scale: Recent Advances in Mass Spectrometry Imaging. Annu. Rev. Anal. Chem 2019, 12, 201.

(61). Nunez J; Renslow R; Cliff JB; Anderton CR NanoSIMS for biological applications: Current practices and analyses. Biointerphases 2018, 13, 03B301.

(62). Tian H; Six DA; Krucker T; Leeds JA; Winograd N Subcellular Chemical Imaging of Antibiotics in Single Bacteria Using C60-Secondary Ion Mass Spectrometry. Anal. Chem 2017, 89, 5050. [PubMed: 28332827]

(63). Massonnet P; Heeren RMA A concise tutorial review of TOF-SIMS based molecular and cellular imaging. J. Anal. At. Spectrom 2019, 34, 2217.

(64). Yin L; Zhang Z; Liu Y; Gao Y; Gu J Recent advances in single-cell analysis by mass spectrometry. Analyst 2019, 144, 824. [PubMed: 30334031]

(65). Li H-W; Hua X; Long Y-T Graphene quantum dots enhanced ToF-SIMS for single-cell imaging. Anal. Bioanal. Chem 2019, 411, 4025. [PubMed: 30796482]

(66). Gularyan SK; Gulin AA; Anufrieva KS; Shender V; Shakhparonov MI; Bastola S; Antipova NV; Kovalenko TF; Rubtsov YP; Latyshev YA; Potapov AA; Pavlyukov MS Investigation of inter- and intra-tumoral heterogeneity of glioblastoma using TOF-SIMS. Mol. Cell. Proteomics 2020, 19, 960. [PubMed: 32265293]

(67). Mezger STP; Mingels AMA; Bekers O; Cillero-Pastor B; Heeren RMA Trends in mass spectrometry imaging for cardiovascular diseases. Anal. Bioanal. Chem 2019, 411, 3709. [PubMed: 30980090]

(68). Mulder IA; Ogrinc Potočnik N; Broos LAM; Prop A; Wermer MJH; Heeren RMA; van den Maagdenberg AMJM Distinguishing core from penumbra by lipid profiles using Mass Spectrometry Imaging in a transgenic mouse model of ischemic stroke. Sci. Rep 2019, 9, 1090. [PubMed: 30705295]

(69). Wiseman JM; Ifa DR; Venter A; Cooks RG Ambient molecular imaging by desorption electrospray ionization mass spectrometry. Nat. Protoc 2008, 3, 517. [PubMed: 18323820]

(70). Wang X; Hou Y; Hou Z; Xiong W; Huang G Mass Spectrometry Imaging of Brain Cholesterol and Metabolites with Trifluoroacetic Acid-Enhanced Desorption Electrospray Ionization. Anal. Chem 2019, 91, 2719. [PubMed: 30645089]

(71). Huang L; Mao X; Sun C; Luo Z; Song X; Li X; Zhang R; Lv Y; Chen J; He J; Abliz Z A graphical data processing pipeline for mass spectrometry imaging-based spatially resolved metabolomics on tumor heterogeneity. Anal. Chim. Acta 2019, 1077, 183. [PubMed: 31307708]

(72). Martin R; Midey A; Olivos H; Shrestha B; Claude E Spatial Mapping of Lipids and Neurotransmitters in Rat Brain Section Using DESI Ion Mobility Mass Spectrometry. J. Biomol Tech 2019, 30, S38.

(73). Nguyen SN; Kyle JE; Dautel SE; Sontag R; Luders T; Corley R; Ansong C; Carson J; Laskin J Lipid Coverage in Nanospray Desorption Electrospray Ionization Mass Spectrometry Imaging of Mouse Lung Tissues. Anal. Chem 2019, 91, 11629. [PubMed: 31412198]

(74). Nagai K; Uranbileg B; Chen Z; Fujioka A; Yamazaki T; Matsumoto Y; Tsukamoto H; Ikeda H; Yatomi Y; Chiba H; Hui S-P; Nakazawa T; Saito R; Koshiba S; Aoki J; Saigusa D; Tomioka Y Identification of novel biomarkers of hepatocellular carcinoma by high-definition mass spectrometry: Ultrahigh-performance liquid chromatography quadrupole time-of-flight mass spectrometry and desorption electrospray ionization mass spectrometry imaging. Rapid Commun. Mass Spectrom 2020, 34, e8551. [PubMed: 31412144]

(75). Liu C; Qi K; Yao L; Xiong Y; Zhang X; Zang J; Tian C; Xu M; Yang J; Lin Z; Lv Y; Xiong W; Pan Y Imaging of Polar and Nonpolar Species Using Compact Desorption Electrospray Ionization/Postphotoionization Mass Spectrometry. Anal. Chem 2019, 91, 6616. [PubMed: 30907581]

(76). Unsihuay D; Qiu J; Swaroop S; Nagornov KO; Kozhinov AN; Tsybin YO; Kuang S; Laskin J Imaging of triglycerides in tissues using nanospray desorption electrospray ionization (Nano-DESI) mass spectrometry. Int. J. Mass Spectrom 2020, 448, 116269. [PubMed: 32863736]

(77). Feider CL; Woody S; Ledet S; Zhang J; Sebastian K; Breen MT; Eberlin LS Molecular Imaging of Endometriosis Tissues using Desorption Electrospray Ionization Mass Spectrometry. Sci. Rep 2019, 9, 15690. [PubMed: 31666535]

(78). Banerjee S; Wong AC-Y; Yan X; Wu B; Zhao H; Tibshirani RJ; Zare RN; Brooks JD Early detection of unilateral ureteral obstruction by desorption electrospray ionization mass spectrometry. Sci. Rep 2019, 9, 11007. [PubMed: 31358807]

(79). Tamura K; Horikawa M; Sato S; Miyake H; Setou M Discovery of lipid biomarkers correlated with disease progression in clear cell renal cell carcinoma using desorption electrospray ionization imaging mass spectrometry. Oncotarget 2019, 10, 1688. [PubMed: 30899441]

(80). Zheng Q; Ruan X; Tian Y; Hu J; Wan N; Lu W; Xu X; Wang G; Hao H; Ye H Ligand–protein target screening from cell matrices using reactive desorption electrospray ionization-mass spectrometry via a native-denatured exchange approach. Analyst 2019, 144, 512. [PubMed: 30489587]

(81). Alfaro CM; Pirro V; Keating MF; Hattab EM; Cooks RG; Cohen-Gadol AA J. Neurosurg 2020, 132, 180.

(82). DeHoog RJ; Zhang J; Alore E; Lin JQ; Yu W; Woody S; Almendariz C; Lin M; Engelsman AF; Sidhu SB; Tibshirani R; Suliburk J; Eberlin LS Preoperative metabolic classification of thyroid nodules using mass spectrometry imaging of fine-needle aspiration biopsies. Proc. Natl. Acad. Sci. U. S. A 2019, 116, 21401. [PubMed: 31591199]

(83). Sans M; Gharpure K; Tibshirani R; Zhang J; Liang L; Liu J; Young JH; Dood RL; Sood AK; Eberlin LS Metabolic Markers and Statistical Prediction of Serous Ovarian Cancer Aggressiveness by Ambient Ionization Mass Spectrometry Imaging. Cancer Res 2017, 77, 2903. [PubMed: 28416487]

(84). Zhang J; Rector J; Lin JQ; Young JH; Sans M; Katta N; Giese N; Yu W; Nagi C; Suliburk J; Liu J; Bensussan A; DeHoog RJ; Garza KY; Ludolph B; Sorace AG; Syed A; Zahedivash A; Milner TE; Eberlin LS Nondestructive tissue analysis for ex vivo and in vivo cancer diagnosis using a handheld mass spectrometry system. Sci. Transl. Med 2017, 9, eaan3968. [PubMed: 28878011]

(85). Feider CL; Krieger A; DeHoog RJ; Eberlin LS Ambient Ionization Mass Spectrometry: Recent Developments and Applications. Anal. Chem 2019, 91, 4266. [PubMed: 30790515]

(86). Hall OM; Peer CJ; Figg WD Tissue preservation with mass spectroscopic analysis: Implications for cancer diagnostics. Cancer Biol. Ther 2018, 19, 953. [PubMed: 29771621]

(87). Sans M; Zhang J; Lin JQ; Feider CL; Giese N; Breen MT; Sebastian K; Liu J; Sood AK; Eberlin LS Performance of the MasSpec Pen for Rapid Diagnosis of Ovarian Cancer. Clin. Chem 2019, 65, 674. [PubMed: 30770374]

(88). St John ER; Balog J; McKenzie JS; Rossi M; Covington A; Muirhead L; Bodai Z; Rosini F; Speller AV; Shousha S Rapid evaporative ionisation mass spectrometry of electrosurgical vapours for the identification of breast pathology: towards an intelligent knife for breast cancer surgery. Breast Cancer Res 2017, 19, 59. [PubMed: 28535818]

(89). Tran NH; Zhang X; Xin L; Shan B; Li M De novo peptide sequencing by deep learning. Proc. Natl. Acad. Sci. U. S. A 2017, 114, 8247. [PubMed: 28720701]

(90). Kumar D; Yadav AK; Dash D In Proteome Bioinformatics; Springer: 2017; p 17.

(91). Jadid SE; Touahni R; Moussa A In Proceedings of the New Challenges in Data Sciences: Acts of the Second Conference of the Moroccan Classification Society; Association for Computing Machinery: Kenitra, Morocco, 2019; Article 4.

(92). El-Aneed A; Cohen A; Banoub J Mass Spectrometry, Review of the Basics: Electrospray, MALDI, and Commonly Used Mass Analyzers. Appl. Spectrosc. Rev 2009, 44, 210.

(93). Korte AR; Yagnik GB; Feenstra AD; Lee YJ Multiplex MALDI-MS imaging of plant metabolites using a hybrid MS system. Methods Mol. Biol 2015, 1203, 49. [PubMed: 25361666]

(94). Ellis SR; Paine MRL; Eijkel GB; Pauling JK; Husen P; Jervelund MW; Hermansson M; Ejsing CS; Heeren RMA Automated, parallel mass spectrometry imaging and structural identification of lipids. Nat. Methods 2018, 15, 515. [PubMed: 29786091]

(95). Comi TJ; Neumann EK; Do TD; Sweedler JV microMS: A Python Platform for Image-Guided Mass Spectrometry Profiling. J. Am. Soc. Mass Spectrom 2017, 28, 1919. [PubMed: 28593377]

(96). Comi TJ; Makurath MA; Philip MC; Rubakhin SS; Sweedler JV MALDI MS Guided Liquid Microjunction Extraction for Capillary Electrophoresis–Electrospray Ionization MS Analysis of Single Pancreatic Islet Cells. Anal. Chem 2017, 89, 7765. [PubMed: 28636327]

(97). Ryan DJ; Patterson NH; Putnam NE; Wilde AD; Weiss A; Perry WJ; Cassat JE; Skaar EP; Caprioli RM; Spraggins JM MicroLESA: Integrating Autofluorescence Microscopy, In Situ Micro-Digestions, and Liquid Extraction Surface Analysis for High Spatial Resolution Targeted Proteomic Studies. Anal. Chem 2019, 91, 7578. [PubMed: 31149808]

(98). Ryan DJ; Nei D; Prentice BM; Rose KL; Caprioli RM; Spraggins JM Protein identification in imaging mass spectrometry through spatially targeted liquid micro-extractions. Rapid Commun. Mass Spectrom 2018, 32, 442. [PubMed: 29226434]

(99). Delcourt V; Franck J; Quanico J; Gimeno J-P; Wisztorski M; Raffo-Romero A; Kobeissy F; Roucou X; Salzet M; Fournier I Spatially-Resolved Top-down Proteomics Bridged to MALDI MS Imaging Reveals the Molecular Physiome of Brain Regions. Mol. Cell. Proteomics 2018, 17, 357. [PubMed: 29122912]

(100). Kompauer M; Heiles S; Spengler B Atmospheric pressure MALDI mass spectrometry imaging of tissues and cells at 1.4-μm lateral resolution. Nat. Methods 2017, 14, 90. [PubMed: 27842060]

(101). Prentice BM; McMillen JC; Caprioli RM Multiple TOF/TOF events in a single laser shot for multiplexed lipid identifications in MALDI imaging mass spectrometry. Int. J. Mass Spectrom 2019, 437, 30. [PubMed: 30906202]

(102). Pasilis SP; Kertesz V; Van Berkel GJ; Schulz M; Schorcht S HPTLC/DESI-MS imaging of tryptic protein digests separated in two dimensions. J. Mass Spectrom 2008, 43, 1627. [PubMed: 18563861]

(103). Fisher GL Structural Assessment of (Sub-)Monolayer Coatings in Device Processing at High Spatial Resolving Power by TOF-SIMS Tandem MS Imaging. Microsc. Microanal 2019, 25, 732.

(104). Angerer TB; Velickovic D; Nicora CD; Kyle JE; Graham DJ; Anderton C; Gamble LJ Exploiting the Semidestructive Nature of Gas Cluster Ion Beam Time-of-Flight Secondary Ion Mass Spectrometry Imaging for Simultaneous Localization and Confident Lipid Annotations. Anal. Chem 2019, 91, 15073. [PubMed: 31659904]

(105). Bruinen AL; Fisher GL; Heeren RM In Imaging Mass Spectrometry; Springer: 2017; p 165.

(106). Ogrinc Potočnik N; Fisher GL; Prop A; Heeren RMA Sequencing and Identification of Endogenous Neuropeptides with Matrix-Enhanced Secondary Ion Mass Spectrometry Tandem Mass Spectrometry. Anal. Chem 2017, 89, 8223. [PubMed: 28753276]

(107). Fu T; Houël E; Amusant N; Touboul D; Genta-Jouve G; Della-Negra S; Fisher GL; Brunelle A; Duplais C Biosynthetic investigation of γ-lactones in Sextonia rubra wood using in situ TOF-SIMS MS/MS imaging to localize and characterize biosynthetic intermediates. Sci. Rep 2019, 9, 1928. [PubMed: 30760744]

(108). Sugiura Y; Zaima N; Setou M; Ito S; Yao I Visualization of acetylcholine distribution in central nervous system tissue sections by tandem imaging mass spectrometry. Anal. Bioanal. Chem 2012, 403, 1851. [PubMed: 22526660]

(109). Takeo E; Sugiura Y; Uemura T; Nishimoto K; Yasuda M; Sugiyama E; Ohtsuki S; Higashi T; Nishikawa T; Suematsu M; Fukusaki E; Shimma S Tandem Mass Spectrometry Imaging Reveals Distinct Accumulation Patterns of Steroid Structural Isomers in Human Adrenal Glands. Anal. Chem 2019, 91, 8918. [PubMed: 31204806]

(110). Sisley EK; Ujma J; Palmer M; Giles K; Fernandez-Lima FA; Cooper HJ LESA Cyclic Ion Mobility Mass Spectrometry of Intact Proteins from Thin Tissue Sections. Anal. Chem 2020, 92, 6321. [PubMed: 32271006]

(111). Desbenoit N; Walch A; Spengler B; Brunelle A; Römpp A Correlative mass spectrometry imaging, applying time-of-flight secondary ion mass spectrometry and atmospheric pressure matrix-assisted laser desorption/ionization to a single tissue section. Rapid Commun. Mass Spectrom 2018, 32, 159. [PubMed: 29105220]

(112). Erne R; Bernard L; Steuer AE; Baumgartner MR; Kraemer T Hair Analysis: Contamination versus Incorporation from the Circulatory System—Investigations on Single Hair Samples Using Time-of-Flight Secondary Ion Mass Spectrometry and Matrix-Assisted Laser Desorption/Ionization Mass Spectrometry. Anal. Chem 2019, 91, 4132. [PubMed: 30816705]

(113). Lanni EJ; Masyuko RN; Driscoll CM; Aerts JT; Shrout JD; Bohn PW; Sweedler JV MALDI-guided SIMS: Multiscale Imaging of Metabolites in Bacterial Biofilms. Anal. Chem 2014, 86, 9139. [PubMed: 25133532]

(114). Dowlatshahi Pour M; Malmberg P; Ewing A An investigation on the mechanism of sublimed DHB matrix on molecular ion yields in SIMS imaging of brain tissue. Anal. Bioanal. Chem 2016, 408, 3071. [PubMed: 26922337]

(115). Cai L; Sheng L; Xia M; Li Z; Zhang S; Zhang X; Chen H Graphene Oxide as a Novel Evenly Continuous Phase Matrix for TOF-SIMS. J. Am. Soc. Mass Spectrom 2017, 28, 399. [PubMed: 27981442]

(116). Škrášková K; Claude E; Jones EA; Towers M; Ellis SR; Heeren RMA Enhanced capabilities for imaging gangliosides in murine brain with matrix-assisted laser desorption/ionization and desorption electrospray ionization mass spectrometry coupled to ion mobility separation. Methods 2016, 104, 69. [PubMed: 26922843]

(117). Eberlin LS; Liu X; Ferreira CR; Santagata S; Agar NYR; Cooks RG Desorption Electrospray Ionization then MALDI Mass Spectrometry Imaging of Lipid and Protein Distributions in Single Tissue Sections. Anal. Chem 2011, 83, 8366. [PubMed: 21975048]

(118). Prosen H; Zupančič-Kralj L Solid-phase microextraction. TrAC, Trends Anal. Chem 1999, 18, 272.

(119). Gómez-Ríos GA; Mirabelli MF Solid Phase Microextraction-mass spectrometry: Metanoia. TrAC, Trends Anal. Chem 2019, 112, 201.

(120). Psillakis E; Kalogerakis N Developments in liquid-phase microextraction. TrAC, Trends Anal. Chem 2003, 22, 565.

(121). Wang C-H; Su H; Chou J-H; Lin J-Y; Huang M-Z; Lee C-W; Shiea J Multiple solid phase microextraction combined with ambient mass spectrometry for rapid and sensitive detection of trace chemical compounds in aqueous solution. Anal. Chim. Acta 2020, 1107, 101. [PubMed: 32200883]

(122). Van Berkel GJ; Kertesz V; Koeplinger KA; Vavrek M; Kong A-NT Liquid microjunction surface sampling probe electrospray mass spectrometry for detection of drugs and metabolites in thin tissue sections. J. Mass Spectrom 2008, 43, 500. [PubMed: 18035855]

(123). Eikel D; Vavrek M; Smith S; Bason C; Yeh S; Korfmacher WA; Henion JD Liquid extraction surface analysis mass spectrometry (LESA-MS) as a novel profiling tool for drug distribution and metabolism analysis: the terfenadine example. Rapid Commun. Mass Spectrom 2011, 25, 3587. [PubMed: 22095508]

(124). Cahill JF; Khalid M; Retterer ST; Walton CL; Kertesz V In Situ Chemical Monitoring and Imaging of Contents within Microfluidic Devices Having a Porous Membrane Wall Using Liquid Microjunction Surface Sampling Probe Mass Spectrometry. J. Am. Soc. Mass Spectrom 2020, 31, 832. [PubMed: 32233378]

(125). Quanico J; Franck J; Cardon T; Leblanc E; Wisztorski M; Salzet M; Fournier I NanoLC-MS coupling of liquid microjunction microextraction for on-tissue proteomic analysis. Biochim. Biophys. Acta, Proteins Proteomics 2017, 1865, 891. [PubMed: 27836619]

(126). May JC; Goodwin CR; Lareau NM; Leaptrot KL; Morris CB; Kurulugama RT; Mordehai A; Klein C; Barry W; Darland E; Overney G; Imatani K; Stafford GC; Fjeldsted JC; McLean JA Conformational Ordering of Biomolecules in the Gas Phase: Nitrogen Collision Cross Sections Measured on a Prototype High Resolution Drift Tube Ion Mobility-Mass Spectrometer. Anal. Chem 2014, 86, 2107. [PubMed: 24446877]

(127). Valentine SJ; Koeniger SL; Clemmer DE A Split-Field Drift Tube for Separation and Efficient Fragmentation of Biomolecular Ions. Anal. Chem 2003, 75, 6202. [PubMed: 14616002]

(128). Zhong Y; Hyung S-J; Ruotolo BT Characterizing the resolution and accuracy of a second-generation traveling-wave ion mobility separator for biomolecular ions. Analyst 2011, 136, 3534. [PubMed: 21445388]

(129). Shvartsburg AA; Smith RD Fundamentals of Traveling Wave Ion Mobility Spectrometry. Anal. Chem 2008, 80, 9689. [PubMed: 18986171]

(130). Purves RW; Guevremont R Electrospray Ionization High-Field Asymmetric Waveform Ion Mobility Spectrometry–Mass Spectrometry. Anal. Chem 1999, 71, 2346. [PubMed: 21662783]

(131). Kolakowski BM; Mester Z Review of applications of high-field asymmetric waveform ion mobility spectrometry (FAIMS) and differential mobility spectrometry (DMS). Analyst 2007, 132, 842. [PubMed: 17710259]

(132). Guevremont R High-field asymmetric waveform ion mobility spectrometry: A new tool for mass spectrometry. Journal of Chromatography A 2004, 1058, 3. [PubMed: 15595648]

(133). Fernandez-Lima F; Kaplan DA; Suetering J; Park MA Gas-phase separation using a trapped ion mobility spectrometer. Int. J. Ion Mobility Spectrom 2011, 14, 93.

(134). Michelmann K; Silveira JA; Ridgeway ME; Park MA Fundamentals of Trapped Ion Mobility Spectrometry. J. Am. Soc. Mass Spectrom 2015, 26, 14. [PubMed: 25331153]

(135). Groessl M; Graf S; Knochenmuss R High resolution ion mobility-mass spectrometry for separation and identification of isomeric lipids. Analyst 2015, 140, 6904. [PubMed: 26312258]

(136). Ridgeway ME; Lubeck M; Jordens J; Mann M; Park MA Trapped ion mobility spectrometry: A short review. Int. J. Mass Spectrom 2018, 425, 22.

(137). Fernandez-Lima F; Kaplan D; Park M Note: Integration of trapped ion mobility spectrometry with mass spectrometry. Rev. Sci. Instrum 2011, 82, 126106. [PubMed: 22225261]

(138). Adams KJ; Montero D; Aga D; Fernandez-Lima F Isomer separation of polybrominated diphenyl ether metabolites using nanoESI-TIMS-MS. Int. J. Ion Mobility Spectrom 2016, 19, 69.

(139). Ibrahim YM; Hamid AM; Deng L; Garimella SV; Webb IK; Baker ES; Smith RD New frontiers for mass spectrometry based upon structures for lossless ion manipulations. Analyst 2017, 142, 1010. [PubMed: 28262893]

(140). Deng L; Ibrahim YM; Baker ES; Aly NA; Hamid AM; Zhang X; Zheng X; Garimella SVB; Webb IK; Prost SA; Sandoval JA; Norheim RV; Anderson GA; Tolmachev AV; Smith RD Ion Mobility Separations of Isomers based upon Long Path Length Structures for Lossless Ion Manipulations Combined with Mass Spectrometry. ChemistrySelect 2016, 1, 2396. [PubMed: 28936476]

(141). Giles K; Ujma J; Wildgoose J; Pringle S; Richardson K; Langridge D; Green M A Cyclic Ion Mobility-Mass Spectrometry System. Anal. Chem 2019, 91, 8564. [PubMed: 31141659]

(142). Deng L; Webb IK; Garimella SV; Hamid AM; Zheng X; Norheim RV; Prost SA; Anderson GA; Sandoval JA; Baker ES Serpentine ultralong path with extended routing (SUPER) high resolution traveling wave ion mobility-MS using structures for lossless ion manipulations. Anal. Chem 2017, 89, 4628. [PubMed: 28332832]

(143). Woods AS; Ugarov M; Egan T; Koomen J; Gillig KJ; Fuhrer K; Gonin M; Schultz JA Lipid/Peptide/Nucleotide Separation with MALDI-Ion Mobility-TOF MS. Anal. Chem 2004, 76, 2187. [PubMed: 15080727]

(144). McLean JA; Ridenour WB; Caprioli RM Profiling and imaging of tissues by imaging ion mobility-mass spectrometry. J. Mass Spectrom 2007, 42, 1099. [PubMed: 17621390]

(145). Spraggins JM; Djambazova KV; Rivera ES; Migas LG; Neumann EK; Fuetterer A; Suetering J; Goedecke N; Ly A; Van de Plas R; Caprioli RM High-Performance Molecular Imaging with MALDI Trapped Ion-Mobility Time-of-Flight (timsTOF) Mass Spectrometry. Anal. Chem 2019, 91, 14552. [PubMed: 31593446]

(146). Griffiths RL; Hughes JW; Abbatiello SE; Belford MW; Styles IB; Cooper HJ Comprehensive LESA Mass Spectrometry Imaging of Intact Proteins by Integration of Cylindrical FAIMS. Anal. Chem 2020, 92, 2885. [PubMed: 31967787]

(147). Klingner N; Heller R; Hlawacek G; Facsko S; von Borany J Time-of-flight secondary ion mass spectrometry in the helium ion microscope. Ultramicroscopy 2019, 198, 10. [PubMed: 30612043]

(148). Araki T The history of optical microscope. Mechanical Engineering Reviews 2017, 4, 16.

(149). van Helvoort T; Sankaran N How Seeing Became Knowing: The Role of the Electron Microscope in Shaping the Modern Definition of Viruses. Journal of the History of Biology 2019, 52, 125. [PubMed: 29926225]

(150). Murphy RF Building cell models and simulations from microscope images. Methods 2016, 96, 33. [PubMed: 26484733]

(151). Sahl SJ; Hell SW; Jakobs S Fluorescence nanoscopy in cell biology. Nat. Rev. Mol. Cell Biol 2017, 18, 685. [PubMed: 28875992]

(152). Kumarasinghe MP; Bourke MJ; Brown I; Draganov PV; McLeod D; Streutker C; Raftopoulos S; Ushiku T; Lauwers GY Pathological assessment of endoscopic resections of the gastrointestinal tract: a comprehensive clinicopathologic review. Mod. Pathol 2020, 33, 986. [PubMed: 31907377]

(153). Deschaine MA; Lehman JS The interface reaction pattern in the skin: an integrated review of clinical and pathological features. Hum. Pathol 2019, 91, 86. [PubMed: 31278974]

(154). Picard C; Orbach D; Carton M; Brugieres L; Renaudin K; Aubert S; Berrebi D; Galmiche L; Dujardin F; Leblond P; Thomas-Teinturier C; Dijoud F Revisiting the role of the pathological grading in pediatric adrenal cortical tumors: results from a national cohort study with pathological review. Mod. Pathol 2019, 32, 546. [PubMed: 30401946]

(155). Sun C; Liu W; Mu Y; Wang X 1,1′-binaphthyl-2,2′-diamine as a novel MALDI matrix to enhance the in situ imaging of metabolic heterogeneity in lung cancer. Talanta 2020, 209, 120557. [PubMed: 31892065]

(156). Wang Y; Hinz S; Uckermann O; Hönscheid P; von Schönfels W; Burmeister G; Hendricks A; Ackerman JM; Baretton GB; Hampe J; Brosch M; Schafmayer C; Shevchenko A; Zeissig S Shotgun lipidomics-based characterization of the landscape of lipid metabolism in colorectal cancer. Biochim. Biophys. Acta, Mol. Cell Biol. Lipids 2020, 1865, 158579. [PubMed: 31794862]

(157). Andersen MK; Krossa S; Høiem TS; Buchholz R; Claes BSR; Balluff B; Ellis SR; Richardsen E; Bertilsson H; Heeren RMA; Bathen TF; Karst U; Giskeødegård GF; Tessem M-B Simultaneous Detection of Zinc and Its Pathway Metabolites Using MALDI MS Imaging of Prostate Tissue. Anal. Chem 2020, 92, 3171. [PubMed: 31944670]

(158). Marsilio S; Newman SJ; Estep JS; Giaretta PR; Lidbury JA; Warry E; Flory A; Morley PS; Smoot K; Seeley EH; Powell MJ; Suchodolski JS; Steiner JM Differentiation of lymphocytic-plasmacytic enteropathy and small cell lymphoma in cats using histology-guided mass spectrometry. J. Vet. Intern. Med 2020, 34, 669. [PubMed: 32100916]

(159). Cordeiro FB; Jarmusch AK; León M; Ferreira CR; Pirro V; Eberlin LS; Hallett J; Miglino MA; Cooks RG Mammalian ovarian lipid distributions by desorption electrospray ionization–mass spectrometry (DESI-MS) imaging. Anal. Bioanal. Chem 2020, 412, 1251. [PubMed: 31953714]

(160). Zhang G; Zhang J; DeHoog RJ; Pennathur S; Anderton CR; Venkatachalam MA; Alexandrov T; Eberlin LS; Sharma K DESI-MSI and METASPACE indicates lipid abnormalities and altered mitochondrial membrane components in diabetic renal proximal tubules. Metabolomics 2020, 16, 11. [PubMed: 31925564]

(161). Severiano DLR; Oliveira-Lima OC; Vasconcelos GA; Lemes Marques B; Almeida de Carvalho G; Freitas EMM; Xavier CH; Gomez MV; Pinheiro ACO; Gomez RS; Vaz BG; Pinto MCX Cerebral Lipid Dynamics in Chronic Cerebral Hypoperfusion Model by DESI-MS Imaging. Neuroscience 2020, 426, 1. [PubMed: 31785353]

(162). Basu SS; Regan MS; Randall EC; Abdelmoula WM; Clark AR; Gimenez-Cassina Lopez B; Cornett DS; Haase A; Santagata S; Agar NYR Rapid MALDI mass spectrometry imaging for surgical pathology. npj Precision Oncology 2019, 3, 17. [PubMed: 31286061]

(163). Sun C; Zhang M; Dong H; Liu W; Guo L; Wang X A spatially-resolved approach to visualize the distribution and biosynthesis of flavones in Scutellaria baicalensis Georgi. J. Pharm. Biomed. Anal 2020, 179, 113014. [PubMed: 31812804]

(164). Sun C; Liu W; Ma S; Zhang M; Geng Y; Wang X Development of a high-coverage matrix-assisted laser desorption/ionization mass spectrometry imaging method for visualizing the spatial dynamics of functional metabolites in Salvia miltiorrhiza Bge. Journal of Chromatography A 2020, 1614, 460704. [PubMed: 31753480]

(165). Patterson NH; Tuck M; Lewis A; Kaushansky A; Norris JL; Van de Plas R; Caprioli RM Next Generation Histology-Directed Imaging Mass Spectrometry Driven by Autofluorescence Microscopy. Anal. Chem 2018, 90, 12404. [PubMed: 30274514]

(166). Patterson NH; Tuck M; Van de Plas R; Caprioli RM Advanced Registration and Analysis of MALDI Imaging Mass Spectrometry Measurements through Autofluorescence Microscopy. Anal. Chem 2018, 90, 12395. [PubMed: 30272960]

(167). Goltsev Y; Samusik N; Kennedy-Darling J; Bhate S; Hale M; Vazquez G; Black S; Nolan GP Deep Profiling of Mouse Splenic Architecture with CODEX Multiplexed Imaging. Cell 2018, 174, 968. [PubMed: 30078711]

(168). Eng J; Thibault G; Luoh S-W; Gray JW; Chang YH; Chin K In Biomarkers for Immunotherapy of Cancer: Methods and Protocols; Thurin M, Cesano A, Marincola FM, Eds.; Springer: New York, NY, 2020; p 521.

(169). Rashid R; Gaglia G; Chen Y-A; Lin J-R; Du Z; Maliga Z; Schapiro D; Yapp C; Muhlich J; Sokolov A; Sorger P; Santagata S Highly multiplexed immunofluorescence images and single-cell data of immune markers in tonsil and lung cancer. Sci. Data 2019, 6, 323. [PubMed: 31848351]

(170). Lin T; Jin H; Gong L; Yu R; Sun S; Yang L; Zhang P; Han P; Cheng J; Liu L; Wei Q Surveillance of non-muscle invasive bladder cancer using fluorescence in situ hybridization: Protocol for a systematic review and meta-analysis. Medicine (Philadelphia, PA, U. S.) 2019, 98, e14573.

(171). Miedema J; Andea AA Through the looking glass and what you find there: making sense of comparative genomic hybridization and fluorescence in situ hybridization for melanoma diagnosis. Mod. Pathol 2020, 33, 1318. [PubMed: 32066861]

(172). Schleyer G; Shahaf N; Ziv C; Dong Y; Meoded RA; Helfrich EJN; Schatz D; Rosenwasser S; Rogachev I; Aharoni A; Piel J; Vardi A In plaque-mass spectrometry imaging of a bloom-forming alga during viral infection reveals a metabolic shift towards odd-chain fatty acid lipids. Nature Microbiology 2019, 4, 527.

(173). Solier C; Langen H Antibody-based proteomics and biomarker research—Current status and limitations. Proteomics 2014, 14, 774. [PubMed: 24520068]

(174). Budnik B; Levy E; Harmange G; Slavov N SCoPE-MS: mass spectrometry of single mammalian cells quantifies proteome heterogeneity during cell differentiation. Genome Biol 2018, 19, 161. [PubMed: 30343672]

(175). Kriegsmann K; Longuespée R; Hundemer M; Zgorzelski C; Casadonte R; Schwamborn K; Weichert W; Schirmacher P; Harms A; Kazdal D; Leichsenring J; Stenzinger A; Warth A; Fresnais M; Kriegsmann J; Kriegsmann M Combined Immunohistochemistry after Mass Spectrometry Imaging for Superior Spatial Information. Proteomics: Clin. Appl 2019, 13, 1800035.

(176). Kaya I; Michno W; Brinet D; Iacone Y; Zanni G; Blennow K; Zetterberg H; Hanrieder J Histology-Compatible MALDI Mass Spectrometry Based Imaging of Neuronal Lipids for Subsequent Immunofluorescent Staining. Anal. Chem 2017, 89, 4685. [PubMed: 28318232]

(177). Tominski C; Lösekann-Behrens T; Ruecker A; Hagemann N; Kleindienst S; Mueller CW; Höschen C; Kögel-Knabner I; Kappler A; Behrens S Insights into Carbon Metabolism Provided by Fluorescence *In Situ* Hybridization-Secondary Ion Mass Spectrometry Imaging of an Autotrophic, Nitrate-Reducing, Fe(II)-Oxidizing Enrichment Culture. Appl. Environ. Microbiol 2018, 84, e02166.

(178). Huber K; Kunzke T; Buck A; Langer R; Luber B; Feuchtinger A; Walch A Multimodal analysis of formalin-fixed and paraffin-embedded tissue by MALDI imaging and fluorescence in situ hybridization for combined genetic and metabolic analysis. Lab. Invest 2019, 99, 1535. [PubMed: 31148595]

(179). Dekas AE; Orphan VJ In Methods in Enzymology; Klotz MG, Ed.; Academic Press: 2011; Vol. 486, p 281. [PubMed: 21185440]

(180). Jones MA; Cho SH; Patterson NH; Van de Plas R; Spraggins JM; Boothby MR; Caprioli RM Discovering New Lipidomic Features Using Cell Type Specific Fluorophore Expression to Provide Spatial and Biological Specificity in a Multimodal Workflow with MALDI Imaging Mass Spectrometry. Anal. Chem 2020, 92, 7079. [PubMed: 32298091]

(181). Vanickova L; Guran R; Kollár S; Emri G; Krizkova S; Do T; Heger Z; Zitka O; Adam V Mass spectrometric imaging of cysteine rich proteins in human skin. Int. J. Biol. Macromol 2019, 125, 270. [PubMed: 30517841]

(182). Zhang Z; Sugiura Y; Mune T; Nishiyama M; Terada Y; Mukai K; Nishimoto K Immunohistochemistry for aldosterone synthase CYP11B2 and matrix-assisted laser desorption ionization imaging mass spectrometry for in-situ aldosterone detection. Curr. Opin. Nephrol. Hypertens 2019, 28, 105. [PubMed: 30608249]

(183). Prentice BM; Hart NJ; Phillips N; Haliyur R; Judd A; Armandala R; Spraggins JM; Lowe CL; Boyd KL; Stein RW; Wright CV; Norris JL; Powers AC; Brissova M; Caprioli RM Imaging mass spectrometry enables molecular profiling of mouse and human pancreatic tissue. Diabetologia 2019, 62, 1036. [PubMed: 30955045]

(184). Bien T; Perl M; Machmüller AC; Nitsche U; Conrad A; Johannes L; Müthing J; Soltwisch J; Janssen K-P; Dreisewerd K MALDI-2 Mass Spectrometry and Immunohistochemistry Imaging of Gb3Cer, Gb4Cer, and Further Glycosphingolipids in Human Colorectal Cancer Tissue. Anal. Chem 2020, 92, 7096. [PubMed: 32314902]

(185). Prade VM; Kunzke T; Feuchtinger A; Rohm M; Luber B; Lordick F; Buck A; Walch A De novo discovery of metabolic heterogeneity with immunophenotype-guided imaging mass spectrometry. Mol. Metab 2020, 36, 100953. [PubMed: 32278304]

(186). Rabe J-H; Sammour, D. A; Schulz S; Munteanu B; Ott M; Ochs K; Hohenberger P; Marx A; Platten M; Opitz CA; Ory DS; Hopf C Fourier Transform Infrared Microscopy Enables Guidance

of Automated Mass Spectrometry Imaging to Predefined Tissue Morphologies. Sci. Rep 2018, 8, 313. [PubMed: 29321555]

(187). Jiang H; Kilburn MR; Decelle J; Musat N NanoSIMS chemical imaging combined with correlative microscopy for biological sample analysis. Curr. Opin. Biotechnol 2016, 41, 130. [PubMed: 27506876]

(188). Lovrić J; Dunevall J; Larsson A; Ren L; Andersson S; Meibom A; Malmberg P; Kurczy ME; Ewing AG Nano Secondary Ion Mass Spectrometry Imaging of Dopamine Distribution Across Nanometer Vesicles. ACS Nano 2017, 11, 3446. [PubMed: 27997789]

(189). Liu W; Huang L; Komorek R; Handakumbura PP; Zhou Y; Hu D; Engelhard MH; Jiang H; Yu X-Y; Jansson C; Zhu Z Correlative surface imaging reveals chemical signatures for bacterial hotspots on plant roots. Analyst 2020, 145, 393. [PubMed: 31789324]

(190). Strnad Š; Pražienková V; Sýkora D; Cvačka J; Maletínská L; Popelová A; Vrkoslav V The use of 1,5-diaminonaphthalene for matrix-assisted laser desorption/ionization mass spectrometry imaging of brain in neurodegenerative disorders. Talanta 2019, 201, 364. [PubMed: 31122436]

(191). Yang H; Su R; Wishnok JS; Liu N; Chen C; Liu S; Tannenbaum SR Magnetic silica nanoparticles for use in matrix-assisted laser desorption ionization mass spectrometry of labile biomolecules such as oligosaccharides, amino acids, peptides and nucleosides. Microchim. Acta 2019, 186, 104.

(192). Baker MJ; Trevisan J; Bassan P; Bhargava R; Butler HJ; Dorling KM; Fielden PR; Fogarty SW; Fullwood NJ; Heys KA; Hughes C; Lasch P; Martin-Hirsch PL; Obinaju B; Sockalingum GD; Sulé-Suso J; Strong RJ; Walsh MJ; Wood BR; Gardner P; Martin FL Using Fourier transform IR spectroscopy to analyze biological materials. Nat. Protoc 2014, 9, 1771. [PubMed: 24992094]

(193). Masyuko R; Lanni EJ; Sweedler JV; Bohn PW Correlated imaging – a grand challenge in chemical analysis. Analyst 2013, 138, 1924. [PubMed: 23431559]

(194). Rinia HA; Burger KNJ; Bonn M; Müller M Quantitative Label-Free Imaging of Lipid Composition and Packing of Individual Cellular Lipid Droplets Using Multiplex CARS Microscopy. Biophys. J 2008, 95, 4908. [PubMed: 18689461]

(195). Le TT; Duren HM; Slipchenko MN; Hu C-D; Cheng J-X Label-free quantitative analysis of lipid metabolism in living Caenorhabditis elegans. J. Lipid Res 2010, 51, 672. [PubMed: 19776402]

(196). Li J; Condello S; Thomes-Pepin J; Ma X; Xia Y; Hurley TD; Matei D; Cheng J-X Lipid Desaturation Is a Metabolic Marker and Therapeutic Target of Ovarian Cancer Stem Cells. Cell Stem Cell 2017, 20, 303. [PubMed: 28041894]

(197). Tipping WJ; Lee M; Serrels A; Brunton VG; Hulme AN Stimulated Raman scattering microscopy: an emerging tool for drug discovery. Chem. Soc. Rev 2016, 45, 2075. [PubMed: 26839248]

(198). Meister K; Niesel J; Schatzschneider U; Metzler-Nolte N; Schmidt DA; Havenith M Label-Free Imaging of Metal–Carbonyl Complexes in Live Cells by Raman Microspectroscopy. Angew. Chem., Int. Ed 2010, 49, 3310.

(199). Yamakoshi H; Dodo K; Palonpon A; Ando J; Fujita K; Kawata S; Sodeoka M Alkyne-Tag Raman Imaging for Visualization of Mobile Small Molecules in Live Cells. J. Am. Chem. Soc 2012, 134, 20681. [PubMed: 23198907]

(200). Lazaro-Pacheco D; Shaaban AM; Rehman S; Rehman I Raman spectroscopy of breast cancer. Appl. Spectrosc. Rev 2020, 1, 439.

(201). Ralbovsky NM; Lednev IK Raman spectroscopy and chemometrics: A potential universal method for diagnosing cancer. Spectrochim. Acta, Part A 2019, 219, 463.

(202). Wiercigroch E; Szafraniec E; Czamara K; Pacia MZ; Majzner K; Kochan K; Kaczor A; Baranska M; Malek K Raman and infrared spectroscopy of carbohydrates: A review. Spectrochim. Acta, Part A 2017, 185, 317.

(203). Gautam R; Vanga S; Ariese F; Umapathy S Review of multidimensional data processing approaches for Raman and infrared spectroscopy. EPJ. Techniques and Instrumentation 2015, 2, 8.

(204). Lasch P; Noda I Two-Dimensional Correlation Spectroscopy for Multimodal Analysis of FT-IR, Raman, and MALDI-TOF MS Hyperspectral Images with Hamster Brain Tissue. Anal. Chem 2017, 89, 5008. [PubMed: 28365985]

(205). Tai T; Karácsony O; Bocharova V; Van Berkel GJ; Kertesz V Topographical and Chemical Imaging of a Phase Separated Polymer Using a Combined Atomic Force Microscopy/Infrared Spectroscopy/Mass Spectrometry Platform. Anal. Chem 2016, 88, 2864. [PubMed: 26890087]

(206). Balbekova A; Lohninger H; van Tilborg GAF; Dijkhuizen RM; Bonta M; Limbeck A; Lendl B; Al-Saad KA; Ali M; Celikic M; Ofner J Fourier Transform Infrared (FT-IR) and Laser Ablation Inductively Coupled Plasma–Mass Spectrometry (LA-ICP-MS) Imaging of Cerebral Ischemia: Combined Analysis of Rat Brain Thin Cuts Toward Improved Tissue Classification. Appl. Spectrosc 2018, 72, 241. [PubMed: 28905634]

(207). Neumann EK; Comi TJ; Spegazzini N; Mitchell JW; Rubakhin SS; Gillette MU; Bhargava R; Sweedler JV Multimodal Chemical Analysis of the Brain by High Mass Resolution Mass Spectrometry and Infrared Spectroscopic Imaging. Anal. Chem 2018, 90, 11572. [PubMed: 30188687]

(208). Chisanga M; Linton D; Muhamadali H; Ellis DI; Kimber RL; Mironov A; Goodacre R Rapid differentiation of Campylobacter jejuni cell wall mutants using Raman spectroscopy, SERS and mass spectrometry combined with chemometrics. Analyst 2020, 145, 1236. [PubMed: 31776524]

(209). Dunham SJB; Ellis JF; Baig NF; Morales-Soto N; Cao T; Shrout JD; Bohn PW; Sweedler JV Quantitative SIMS Imaging of Agar-Based Microbial Communities. Anal. Chem 2018, 90, 5654. [PubMed: 29623707]

(210). Morales-Soto N; Dunham SJB; Baig NF; Ellis JF; Madukoma CS; Bohn PW; Sweedler JV; Shrout JD Spatially dependent alkyl quinolone signaling responses to antibiotics in Pseudomonas aeruginosa swarms. J. Biol. Chem 2018, 293, 9544. [PubMed: 29588364]

(211). Burkhow SJ; Stephens NM; Mei Y; Dueñas ME; Freppon DJ; Ding G; Smith SC; Lee Y-J; Nikolau BJ; Whitham SA; Smith EA Characterizing virus-induced gene silencing at the cellular level with in situ multimodal imaging. Plant Methods 2018, 14, 37. [PubMed: 29849743]

(212). Ali A; Abouleila Y; Shimizu Y; Hiyama E; Watanabe TM; Yanagida T; Germond A Single-Cell Screening of Tamoxifen Abundance and Effect Using Mass Spectrometry and Raman-Spectroscopy. Anal. Chem 2019, 91, 2710. [PubMed: 30664349]

(213). Ryabchykov O; Popp J; Bocklitz T Fusion of MALDI Spectrometric Imaging and Raman Spectroscopic Data for the Analysis of Biological Samples. Front. Chem 2018, 6. DOI: 10.3389/fchem.2018.00257

(214). Bergholt MS; Serio A; McKenzie JS; Boyd A; Soares RF; Tillner J; Chiappini C; Wu V; Dannhorn A; Takats Z; Williams A; Stevens MM Correlated Heterospectral Lipidomics for Biomolecular Profiling of Remyelination in Multiple Sclerosis. ACS Cent. Sci 2018, 4, 39. [PubMed: 29392175]

(215). Bakry R; Rainer M; Huck CW; Bonn GK Protein profiling for cancer biomarker discovery using matrix-assisted laser desorption/ionization time-of-flight mass spectrometry and infrared imaging: A review. Anal. Chim. Acta 2011, 690, 26. [PubMed: 21414433]

(216). Petit VW; Réfrégiers M; Guettier C; Jamme F; Sebanayakam K; Brunelle A; Laprévote O; Dumas P; Le Naour F Multimodal Spectroscopy Combining Time-of-Flight-Secondary Ion Mass Spectrometry, Synchrotron-FT-IR, and Synchrotron-UV Microspectroscopies on the Same Tissue Section. Anal. Chem 2010, 82, 3963. [PubMed: 20387890]

(217). Lohöfer F; Hoffmann L; Buchholz R; Huber K; Glinzer A; Kosanke K; Feuchtinger A; Aichler M; Feuerecker B; Kaissis G; Rummeny EJ; Höltke C; Faber C; Schilling F; Botnar RM; Walch AK; Karst U; Wildgruber M Molecular imaging of myocardial infarction with Gadofluorine P – A combined magnetic resonance and mass spectrometry imaging approach. Heliyon 2018, 4, e00606. [PubMed: 29862367]

(218). Lohöfer F; Buchholz R; Glinzer A; Huber K; Haas H; Kaissis G; Feuchtinger A; Aichler M; Sporns PB; Höltke C; Stölting M; Schilling F; Botnar RM; Kimm MA; Faber C; Walch AK; Zernecke A; Karst U; Wildgruber M Mass Spectrometry Imaging of atherosclerosis-affine Gadofluorine following Magnetic Resonance Imaging. Sci. Rep 2020, 10, 79. [PubMed: 31919465]

(219). Srimany A; George C; Naik HR; Pinto DG; Chandrakumar N; Pradeep T Developmental patterning and segregation of alkaloids in areca nut (seed of Areca catechu) revealed by magnetic resonance and mass spectrometry imaging. Phytochemistry 2016, 125, 35. [PubMed: 26896852]

(220). Verbeeck N; Spraggins JM; Murphy MJM; Wang H.-d.; Deutch AY; Caprioli RM; Van de Plas R Connecting imaging mass spectrometry and magnetic resonance imaging-based anatomical atlases for automated anatomical interpretation and differential analysis. Biochim. Biophys. Acta, Proteins Proteomics 2017, 1865, 967. [PubMed: 28254588]

(221). Marshall DD; Powers R Beyond the paradigm: Combining mass spectrometry and nuclear magnetic resonance for metabolomics. Prog. Nucl. Magn. Reson. Spectrosc 2017, 100, 1. [PubMed: 28552170]

(222). Cassat JE; Moore JL; Wilson KJ; Stark Z; Prentice BM; Van de Plas R; Perry WJ; Zhang Y; Virostko J; Colvin DC; Rose KL; Judd AM; Reyzer ML; Spraggins JM; Grunenwald CM; Gore JC; Caprioli RM; Skaar EP Integrated molecular imaging reveals tissue heterogeneity driving host-pathogen interactions. Sci. Transl. Med 2018, 10, eaan6361. [PubMed: 29540616]

(223). Wang Z; Gerstein M; Snyder M RNA-Seq: a revolutionary tool for transcriptomics. Nat. Rev. Genet 2009, 10, 57. [PubMed: 19015660]

(224). Horgan RP; Kenny LC Omic' technologies: genomics, transcriptomics, proteomics and metabolomics. Obstetrician & Gynaecologist 2011, 13, 189.

(225). Kulkarni A; Anderson AG; Merullo DP; Konopka G Beyond bulk: a review of single cell transcriptomics methodologies and applications. Curr. Opin. Biotechnol 2019, 58, 129. [PubMed: 30978643]

(226). Wang Z; Shi H; Yu S; Zhou W; Li J; Liu S; Deng M; Ma J; Wei Y; Zheng Y; Liu Y Comprehensive transcriptomics, proteomics, and metabolomics analyses of the mechanisms regulating tiller production in low-tillering wheat. Theor. Appl. Genet 2019, 132, 2181. [PubMed: 31020386]

(227). Angelidis I; Simon LM; Fernandez IE; Strunz M; Mayr CH; Greiffo FR; Tsitsiridis G; Ansari M; Graf E; Strom T-M; Nagendran M; Desai T; Eickelberg O; Mann M; Theis FJ; Schiller HB An atlas of the aging lung mapped by single cell transcriptomics and deep tissue proteomics. Nat. Commun 2019, 10, 963. [PubMed: 30814501]

(228). Liessem S; Ragionieri L; Neupert S; Büschges A; Predel R Transcriptomic and Neuropeptidomic Analysis of the Stick Insect, Carausius morosus. J. Proteome Res 2018, 17, 2192. [PubMed: 29701990]

(229). Sung C-C; Chen L; Limbutara K; Jung HJ; Gilmer GG; Yang C-R; Lin S-H; Khositseth S; Chou C-L; Knepper MA RNA-Seq and protein mass spectrometry in microdissected kidney tubules reveal signaling processes initiating lithium-induced nephrogenic diabetes insipidus. Kidney Int 2019, 96, 363. [PubMed: 31146973]

(230). Noble KV; Reyzer ML; Barth JL; McDonald H; Tuck M; Schey KL; Krug EL; Lang H Use of Proteomic Imaging Coupled With Transcriptomic Analysis to Identify Biomolecules Responsive to Cochlear Injury. Front. Mol. Neurosci 2018, 11. DOI: 10.3389/fnmol.2018.00243 [PubMed: 29440988]

(231). Kawashima M; Tokiwa M; Nishimura T; Kawata Y; Sugimoto M; Kataoka TR; Sakurai T; Iwaisako K; Suzuki E; Hagiwara M; Harris AL; Toi M High-resolution imaging mass spectrometry combined with transcriptomic analysis identified a link between fatty acid composition of phosphatidylinositols and the immune checkpoint pathway at the primary tumour site of breast cancer. Br. J. Cancer 2020, 122, 245. [PubMed: 31819188]

(232). Jarvis S; Gethings L; Gadeleta R; Claude E; Winston R; Williamson C; Bevan C In Society for Endocrinology BES 2018; BioScientifica: 2018; Vol. 59.

(233). Dunevall J; Majdi S; Larsson A; Ewing A Vesicle impact electrochemical cytometry compared to amperometric exocytosis measurements. Current Opinion in Electrochemistry 2017, 5, 85. [PubMed: 29218327]

(234). Chen C-C; Cang C; Fenske S; Butz E; Chao Y-K; Biel M; Ren D; Wahl-Schott C; Grimm C Patch-clamp technique to characterize ion channels in enlarged individual endolysosomes. Nat. Protoc 2017, 12, 1639. [PubMed: 28726848]

(235). Leyrer-Jackson JM; Olive MF; Gipson CD In Glutamate Receptors: Methods and Protocols; Burger C, Velardo MJ, Eds.; Springer: New York, NY, 2019; p 107.

(236). Phan NTN; Li X; Ewing AG Measuring synaptic vesicles using cellular electrochemistry and nanoscale molecular imaging. Nature Reviews Chemistry 2017, 1, 0048.

(237). Li K; Liu J; Grovenor CRM; Moore KL NanoSIMS Imaging and Analysis in Materials Science. Annu. Rev. Anal. Chem 2020, 13, 273.

(238). Ranjbari E; Majdi S; Ewing A Analytical Techniques: Shedding Light upon Nanometer-Sized Secretory Vesicles. Trends in Chemistry 2019, 1, 440.

(239). Chadwick GL; Jiménez Otero F; Gralnick JA; Bond DR; Orphan VJ NanoSIMS imaging reveals metabolic stratification within current-producing biofilms. Proc. Natl. Acad. Sci. U. S. A 2019, 116, 20716. [PubMed: 31548422]

(240). Thomen A; Najafinobar N; Penen F; Kay E; Upadhyay PP; Li X; Phan NTN; Malmberg P; Klarqvist M; Andersson S; Kurczy ME; Ewing AG Subcellular Mass Spectrometry Imaging and Absolute Quantitative Analysis across Organelles. ACS Nano 2020, 14, 4316. [PubMed: 32239916]

(241). Larsson A; Majdi S; Oleinick A; Svir I; Dunevall J; Amatore C; Ewing AG Intracellular Electrochemical Nano-measurements Reveal that Exocytosis of Molecules at Living Neurons is Subquantal and Complex. Angew. Chem., Int. Ed 2020, 59, 6711.

(242). Baker LA; Jagdale GS On the intersection of electrochemistry and mass spectrometry. Current Opinion in Electrochemistry 2019, 13, 140. [PubMed: 33981910]

(243). Lin L-E; Chen C-L; Huang Y-C; Chung H-H; Lin C-W; Chen K-C; Peng Y-J; Ding S-T; Wang M-Y; Shen T-L; Hsu C-C Precision biomarker discovery powered by microscopy image fusion-assisted high spatial resolution ambient ionization mass spectrometry imaging. Anal. Chim. Acta 2020, 1100, 75. [PubMed: 31987155]

(244). Van de Plas R; Yang J; Spraggins J; Caprioli RM Image fusion of mass spectrometry and microscopy: a multimodality paradigm for molecular tissue mapping. Nat. Methods 2015, 12, 366. [PubMed: 25707028]

(245). Lin L-E; Chen C-L; Huang Y-C; Chung H-H; Lin C-W; Chen K-C; Peng Y-J; Ding S-T; Wang M-Y; Shen T-L; Hsu C-C High Spatial Resolution Ambient Ionization Mass Spectrometry Imaging Using Microscopy Image Fusion Determines Tumor Margins. bioRxiv 2019, 657494.

(246). Vollnhals F; Audinot J-N; Wirtz T; Mercier-Bonin M; Fourquaux I; Schroeppel B; Kraushaar U; Lev-Ram V; Ellisman MH; Eswara S Correlative Microscopy Combining Secondary Ion Mass Spectrometry and Electron Microscopy: Comparison of Intensity–Hue–Saturation and Laplacian Pyramid Methods for Image Fusion. Anal. Chem 2017, 89, 10702. [PubMed: 28901122]

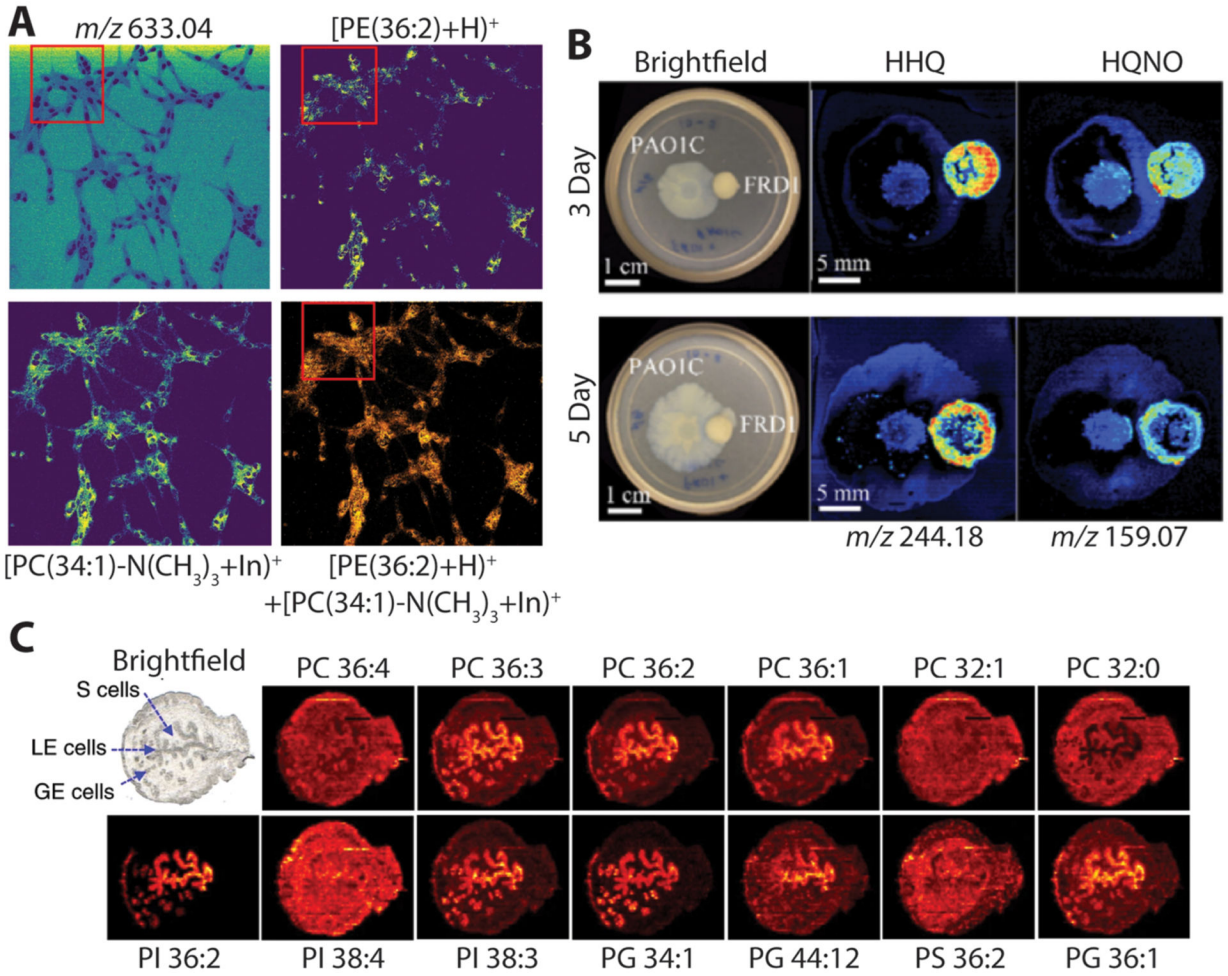

Figure 1.

Selected developments within the IMS community. Image of a Vero B cell culture at 1 μm spatial resolution acquired with transition mode MALDI-2 IMS developed by the Dreiswerd lab (A). Panel A is adapted with permission from ref 47. Copyright 2019 Nature Publishing. SIMS image of a coculture of different *Pseudomonas aeruginosa* strains visualized with different signaling small molecules (B). Panel B is adapted with permission from ref 48 . Copyright 2019 SPIE. Digital Library. Lipid images both positive and negative mode of the mouse uterine tissue using nanoDESI at 10 μm spatial resolution (C). Panel C is adapted with permission from ref 49. Copyright 2019 Nature Publishing.

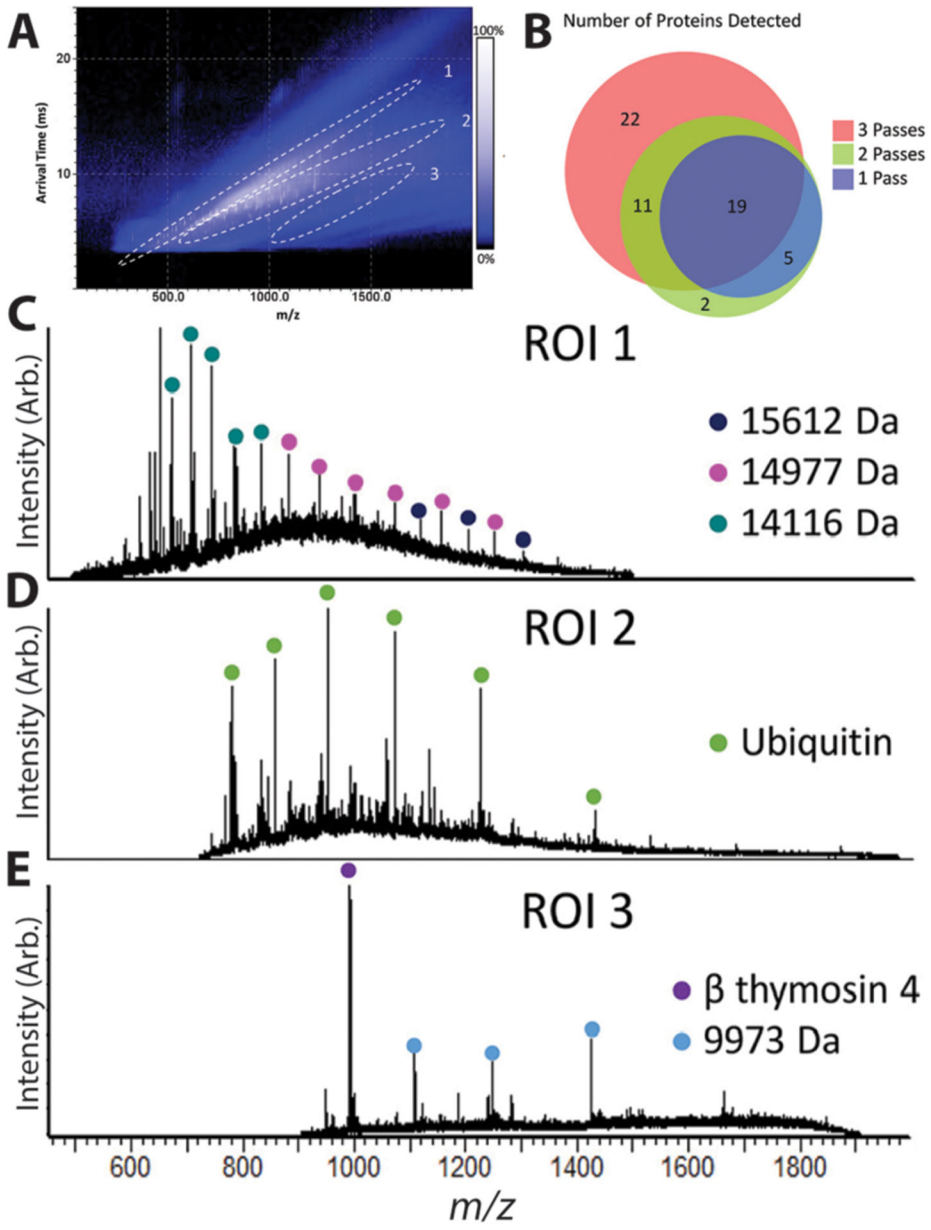

Figure 2.

LESA and cIM analysis of a complex murine kidney protein extract. More proteins are detected after each additional cycle of cIM (A). IM heat map generated from a single cycle of cIM (B), where extracted mass spectra from different trend lines contain different protein signatures (C–E). This figure was adapted with permission from ref 110. Copyright 2020 American Chemical Society.

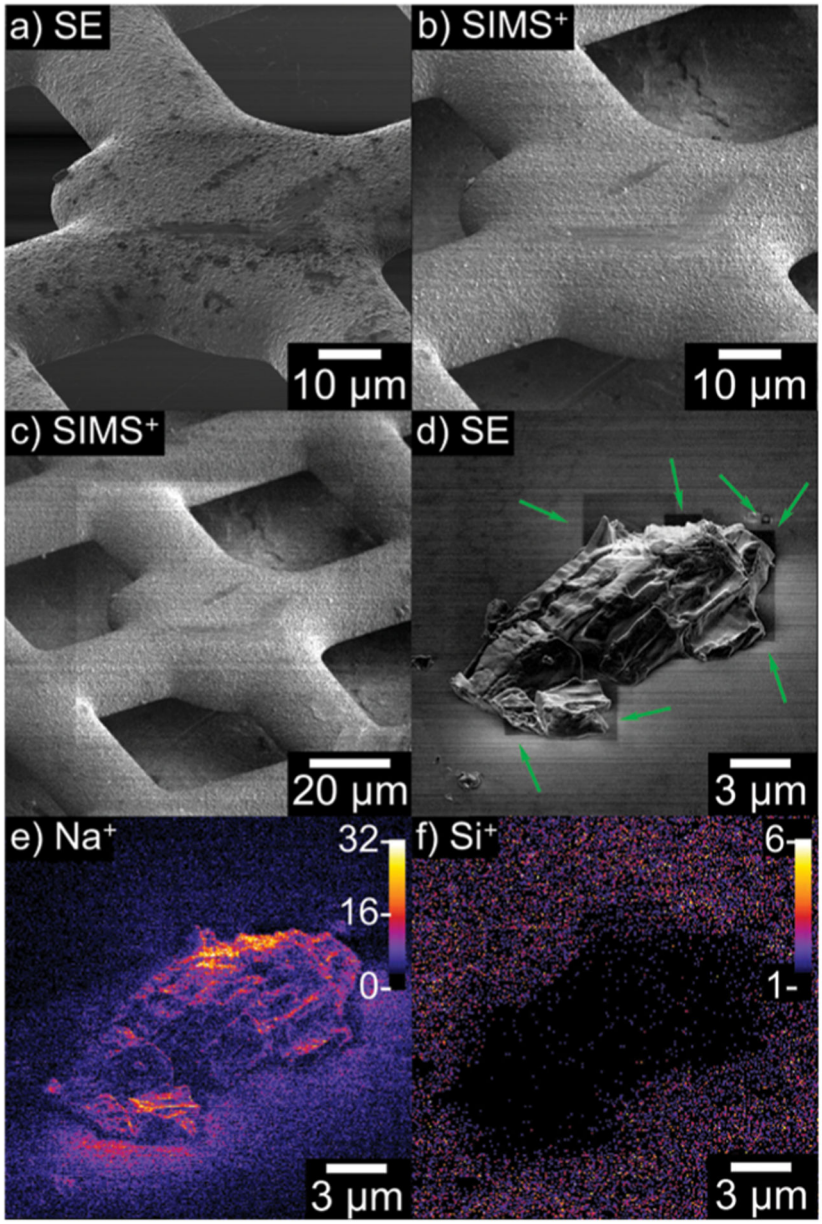

Figure 3.

Images of a TEM grid (A–C) and NaCl salt (D–F) crystal generated from the SIMS helium microscope. The SIMS (B, C, E, and F) images are close to the resolution of the microscopy (A and D), demonstrating the power of this technique. This figure was adapted with permission from ref 147. Copyright 2019 Science Direct.

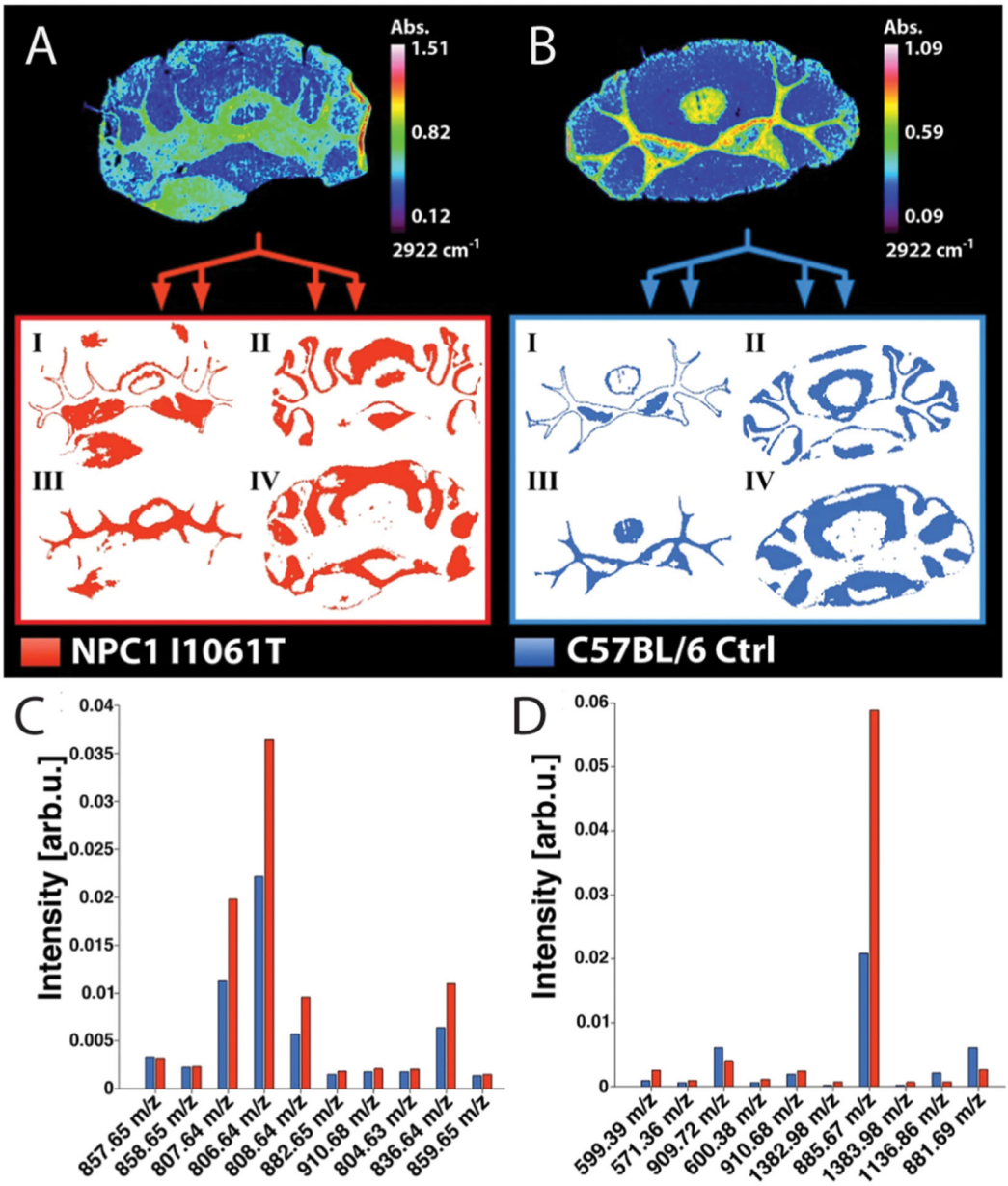

Figure 4.

MALDI IMS lipid profiles obtained after FT-IR generated segmentation. Murine brain is differentially segmented based on absorbance of 2922 cm^{-1} based on disease (A) and control mice (B). Using this segmentation, lipid profiles can be generated for different masks for chemical differentiation (C and D). This figure was adapted with permission from ref 186. Copyright 2018 Nature Publishing.